Title: Frontal Vulnerability vs. Temporal Resilience: Neuro-compensatory mechanisms underline differential language aging trajectories.

Abbreviated title: Frontal-Temporal Reorganization in Language Aging

Authors: Partika Jain[1], Azman Akhter[1], Arpan Banerjee[1]

Affiliation: [1] National Brain Research Centre, NH 8, Manesar, Gurgaon 122052, India

Corresponding Author: Arpan Banerjee (arpan@nbrc.ac.in)

Orcid: https://orcid.org/0009-0008-9892-7459 (Partika Jain)

Orcid: https://orcid.org/0009-0008-1303-2892 (Azman Akhter)

Orcid: https://orcid.org/0000-0002-3725-0463 (Arpan Banerjee)

Number of Pages: 48 (With references and figures)

Number of Figures: 5 main figures, 1 Supplementary figure

Number of Tables: 1 main table, 2 Supplementary tables

Number of Words:

- Abstract: 250
- Introduction: 648
- Discussion: 1588

Conflict of Interest Statement:

The authors declare no competing financial interests

Acknowledgements:

Authors acknowledge the generous support of Computing and Network Facility of NBRC.

Funding: NBRC Core funds (PJ, AK, AB), DBT Dementia Science Programme (AB)

Abstract:

Age-related decline underlies cognitive functions such as sensorimotor control, executive functioning, memory, and language production (LP), whereas language comprehension (LC) tends to remain intact or improve across healthy adult lifespan. Preservation of LC can have structural and functional origins identifiable from key brain regions of the language network (LAN). To investigate this hypothesis, we analyzed the relationships among resting-state brain functional connectivity (rsFC) derived from functional magnetic resonance imaging (fMRI) signals, structural connectivity (SC) derived from diffusion MRI metrices, and behaviour (LC and LP) using a cross-sectional cohort of healthy adults (N = 652; aged 18–88). Six cognitive tasks assessing LC and LP were employed, with neuroimaging measures focused on region-specific connections within the LAN. Using generalized additive mixed models (GAMMs), complex brain-behaviour interactions were identified. Behavioral analyses revealed established age-related dichotomy, LC abilities in vocabulary and proverb comprehension improved and in syntactic and semantic comprehension remained stable, whereas LP tasks, e.g., verbal fluency, picture priming, and tip of tongue exhibited significant decline across the lifespan. SC exhibited decline in both intra- and inter-hemispheric fronto-temporal and frontal lobe connections, contrasted by preserved or enhanced temporal lobe connectivity, supporting a pattern of frontal vulnerability concomitant with temporal resilience. Age-related FC patterns demonstrated overall preservation, reflecting compensatory mechanisms to sustain functional integrity despite structural degradation. GAMM analyses revealed complex relationships between brain connectivity and language performance across age. Thus, integrating knowledge of brain structure, function, and language abilities, we identified the brain network mechanisms associated with dichotomous language behavior along lifespan.

Significance: Understanding how language abilities change with age is crucial for identifying early signs of cognitive decline and developing interventions for aging populations. This study reveals that while the brain's frontal regions-important for language production-become more vulnerable with age, the temporal regions-key for language comprehension-remain resilient or even strengthen. By integrating advanced brain imaging and behavioral testing in a large group of healthy adults, we show that the brain adapts to structural decline through compensatory functional mechanisms. Importantly, disruptions in these patterns could serve as early biomarkers for neurological disorders such as Alzheimer's disease and age-related dementia. By integrating structural, functional, and behavioral measures with advanced modeling, this study offers an accessible framework to guide research and interventions promoting healthy cognitive aging.

Keywords: Language network (LAN), Cognitive aging, Functional connectivity (FC), Structural connectivity (SC), Language comprehension (LC), Language production (LP)

List of Abbreviations

Abbreviations	**Full form**
ACT	Anatomically Constrained Tractography
AIC	Akaike Information Criterion
aCompCor	Anatomical Component-based Noise Correction
ANOVA	Analysis of Variance
ART	Artifact Detection Tool
BA	Brodmann Area
BIC	Bayesian Information Criterion
BOLD	Blood Oxygen Level Dependent
CRUNCH	Compensation-Related Utilization of Neural Circuits Hypothesis
CSF	Cerebrospinal Fluid
CamCAN	Cambridge Centre for Ageing and Neuroscience
DWI	Diffusion Weighted Imaging
EPI	Echo Planar Imaging
FA	Fractional Anisotropy
FBC	Fiber Bundle Capacity
FC	Functional Connectivity
FDR	False Discovery Rate
FOD	Fiber Orientation Distribution
FOV	Field of View
GAMM	Generalized Additive Mixed Model
GLM	General Linear Model
GRAPPA	Generalized Autocalibrating Partially Parallel Acquisition
High_phon	High Phonological similarity
High_sem	High Semantic similarity
IQ	Interquartile
LAN	Language Network
LC	Language Comprehension
LME	Linear Mixed Effects
LP	Language Production
Low_phon	Low Phonological similarity
Low_sem	Low Semantic similarity
MMSE	Mini-Mental State Examination
MNI	Montreal Neurological Institute
MP-PCA	Marchenko-Pastur Principal Component Analysis
MRI	Magnetic Resonance Imaging
MSMT-CSD	Multi-Shell Multi-Tissue Constrained Spherical Deconvolution
PCA	Principal Component Analysis
Proverb	Proverb comprehension
REST	Resting State
ROI	Region of Interest
rs-fMRI	Resting-State Functional Magnetic Resonance Imaging

rsFC	Resting-State Functional Connectivity
RT_Sem_comp	Response Time for Semantically complex sentences
RT_Syn_comp	Response Time for Syntactically complex sentences
RT_high_phon	Response Time for High Phonological similarity
RT_high_sem	Response Time for High Semantic similarity
RT_low_phon	Response Time for Low Phonological similarity
RT_low_sem	Response Time for Low Semantic similarity
SC	Structural Connectivity
STC	Slice-Timing Correction
STG	Superior Temporal Gyrus
Sem_comp	Semantically Complex Sentences
Syn_comp	Syntactically Complex Sentences
TE	Echo Time
TI	Inversion Time
TR	Repetition Time
ToT	Tip of the Tongue
VF	Verbal Fluency
Vocab	Vocabulary

1. Introduction

By 2050, the number of individuals aged over 60 years is projected to triple compared to that in 2000 (United Nations, 2023). Consequently, the prevalence of aging associated cognitive impairments are likely to skyrocket. Hence, in order to characterize pathological aging language abilities are among the primary cognitive functions that are impaired (Mascali et al., 2018; Rafiq et al., 2022; van Boxtel & Lawyer, 2021), adverse processes associated with cognitive aging must be investigated. Although age-related decline is ubiquitous in most cognitive functions, language behavior exhibits an intriguing idiosyncrasy along age-related trajectories which is unanswered in existing literature. With age language production (LP) deteriorates (Burke & Shafto, 2004; Diaz et al., 2016; Zhang & Diaz, 2023a), e.g, older adults experience difficulties such as stuttering, increased retrieval failures, more disfluent speech, and tip-of-the-tongue experiences (Burke & Shafto, 2004; Shafto et al., 2007). In contrast, language comprehension (LC) tend to remain stable or even improve across the lifespan and appear to exhibit unique resilience (Ferré et al., 2019; Salthouse, 2014; Shafto & Tyler, 2014; Sommers et al., 2011; Verhaegen & Poncelet, 2013). Thus, mapping a lifespan-scale developmental trajectory of language abilities on brain structure and function can serve as diagnostic and prognostic marker for neurological disorders such as Alzheimer's and dementia.

Brain mapping using resting-state functional connectivity (rsFC) have emerged as key biomarker capturing up to 80% shared variance with that observed during cognitive tasks in similar areas (Cole et al., 2014). Several studies noticed age-related decline in rsFC across whole brain (Chan et al., 2017; Jiang et al., 2022; Khalilian et al., 2024) and also within the language network (Bolognini & Martin, 2023; Ferré et al., 2019; Zhang et al., 2021; Zhang & Diaz, 2023b). Few have examined rsFC in key language regions in younger and older adults and their relationship with behavioral performance (Ferré et al., 2019; Gertel et al., 2020; Zhang et al., 2021). Importantly, Ferré et al. (2019) revealed age-related decline in rsFC among core language regions forming the language network (LAN) - inferior frontal gyrus (IFG), posterior middle and superior temporal gyrus (MTG, STG), but observed no interaction between FC and language behavior scores, potentially due to their reliance on linear analytical methods. Fewer studies have examined age-related changes in structural connectivity (Damoiseaux, 2017) within LAN. Many of them report age-related decline in several structural measures including white matter volume, gray matter density, cortical thickness, fractional anisotropy (FA) values, and other microstructural properties of white matter tracts (Davis et al., 2009; Fletcher et al., 2018; Henriques et al., 2023; Pistono et al., 2021; Westlye et al., 2010). Specifically in case of language pathways, fronto-temporal connections of the dorsal pathway showed more pronounced

decline in FA values across age (Yang et al., 2014). Houston et al., 2019 showed that white matter integrity, particularly in the frontal-occipital fasciculus (IFOF) and superior longitudinal fasciculus (SLF) may play a crucial role in language performance across the lifespan. However, the study involved a cohort with a mean age of 40, at which global connectivity strength and efficiency among myelin-weighted connections are known to peak (Bosticardo et al., 2024), and hence may not adequately capture the progressive decline in structural connectivity that occurs in later stages of life.

Interestingly, there is ongoing debate in literature whether the neurofunctional changes represent compensatory mechanisms (Cabeza et al., 2018; Davis et al., 2008; Naik et al., 2017) or reflect decline processes such as de-differentiation (Diaz et al., 2014; Li et al., 2001; Zhang & Diaz, 2023a). How do these mechanisms support the dichotomous age-related language behavior trajectories? With the aim of addressing this question by integrating epidemiological, cognitive, neurofunctional, and structural data, the current study utilized a large cohort of healthy individuals with homogeneous age distribution across the adult lifespan and focused on a detailed nonlinear regression analysis of core language network (Branco et al., 2020) with language behaviour across adult lifespan.

2.Materials and Methods

2.1 Participants - The neuroimaging data of cognitively healthy participants (N = 652, age range: 18-88) were obtained from a cross-sectional population-based adult cohort at the Cambridge Centre for Ageing and Neuroscience repository (CamCAN, Stage 2). All participants underwent a series of neuropsychological tests with strict exclusion criteria (Shafto et al., 2014; Taylor et al., 2017), including cognitive impairment (Mini-Mental State Examination [MMSE] score <25, severe memory deficit), communication difficulties (inability to hear 35 dB at 1000 Hz in either ear, poor vision < 20/100, and poor fluency in English), self-reported substance abuse, and experiencing any serious health problems. The education score of each participant was derived by assigning a difficulty level to each education stage provided by the UK government's official website, and then aggregating these values over the participant's lifespan. All participants provided written informed consent, and this study was approved by the Research Ethics Committee of Cambridgeshire 2 (now East of England-Cambridge Central). Subsequently, only participants with complete neuroimaging data comprising T1, resting state fMRI (rs-fMRI), and structural T1 and diffusion weighted MRI (DWI) data were considered in the current study (N = 642). Additionally, 33 participants were excluded because of poor data quality and previously reported artifacts (for details see: Cam-CAN Data Access Portal) Considering that left- and right-handed participants may have hemispherically opposite functional dominance (Knecht et al., 2000) and organization (Tejavibulya et al., 2022), only 558 (Male = 276, age range: 18-88) right-handed participants were included in the subsequent analysis.

2.2 Language behaviour tasks - Six cognitive tests, conducted externally from the scanner, were employed to assess two primary language domains: comprehension and production (LC and LP). These assessments comprised three tasks each for LC and LP. Where applicable, each language task was further categorized into multiple subdomains (accuracy and response time measures) based on linguistic complexity. Specifically, the LC domain included the following subdomains: Vocabulary (Vocab), Proverb comprehension (Proverb), and Sentence comprehension task (Synsem), which was further subdivided into different subdomains: Syntactically complex sentences (Syn_comp), Semantically complex sentences (Sem_comp), and their associated response time measures (RT_Syn_comp and RT_Sem_comp). Accuracy in the Syn_comp task was quantified by deriving a composite measure that integrates accuracy rates across different sentence continuation types. This approach allowed for the evaluation of performance under conditions of both expected and unexpected linguistic structures. Similar composite measures were constructed to assess performance

in the other Synsem subdomains, providing a comprehensive evaluation of syntactic and semantic comprehension abilities.

The LP domain comprised Verbal Fluency (VF), Tip-of-the-Tongue (ToT), and the Picture Priming task, which was further subdivided into different subdomains High Phonological similarity (High_phon), Low Phonological similarity (Low_phon), High Semantic similarity (High_sem), Low Semantic similarity (Low_sem) based on semantic and phonological similarities between prime and the target, and their corresponding response time measures (RT_high_phon, RT_low_phon, RT_high_sem, RT_low_sem). For each of these subdomains, performance was quantified by comparing responses under each condition with a neutral or unrelated baseline condition. For example, accuracy in the High_sem condition was calculated by assessing the improvement in accuracy when the prime was highly semantically related to the target, relative to when the prime and target were unrelated. This approach allowed us to isolate the specific effects of semantic and phonological similarity on production performance. To facilitate consistent interpretation across all measures, the ToT scores and response time variables were sign-reversed so that higher values uniformly indicated better performance. A detailed structure of the tasks and their corresponding subdomains is provided in Table 1, with comprehensive details available in (Shafto et al., 2014).

Table 1. Description of Language behaviour tasks with their descriptive statistics

Language Domain	Language Task	Task Description	Category within the Task	Descriptive Statistics (Mean, SD, Range, Missing)	References
Comprehension	Vocabulary	Brief lexical decision test which involves 60 pairs of items comprising one word and one nonword (e.g., ‘flonty – xylophone’); participant is required to identify the real word.	Vocab	M = 53.49 ± 5.44 Range = (24 – 60) Missing = 0.35%	(Baddeley et al., 1993)
	Proverb comprehension	Read and interpret three English proverbs. Recorded responses were: 0 (incorrect), 1 (concrete), and 2 (abstract).	Proverb	M = 4.5 ± 1.63 Range = (0 – 6) Missing = 3.76%	(Hodges, 1994)
	Sentence Comprehension	Judge grammatical acceptability of partial auditory sentences, which begin with an ambiguous	Semantically Complex (Sem_comp)	M = 0.37 ± 0.32 Range = (-5.96 – 0.79)	(Rodd et al., 2010)

		sentence stem followed by a disambiguating continuation word in a different voice. Ambiguity is either semantic or syntactic, with empirically determined dominant and subordinate interpretations.		Missing = 9.85%	
			Syntactically Complex (Syn_comp)	M = 0.46 ± 0.26	
				Range = (-2.33 – 2.10)	
				Missing = 9.67%	
			Response Time of Sem_comp in milliseconds (RT_Sem_comp)	M = 0.13 ± 0.35	
				Range = (-1.96 – 1.17)	
				Missing = 29.2%	
			Response Time of Syn_comp in milliseconds (RT_Syn_comp)	M = 0.05 ± 0.34	
				Range = (-1 – 1.34)	
				Missing = 30.2%	
Production	Verbal Fluency	Mean scores were calculated for the Letter (phonemic) fluency and Animal (semantic) fluency tasks. Participants had 1 minute to generate as many words as possible.	Verbal Fluency (VF)	M = 58.9 ± 15.4	(Lezak, 1995)
				Range = (18 – 110)	
				Missing = 0.35%	
	Picture Priming	Accuracy and response time in baseline (object presented alone) condition, then when preceded by a prime object that is phonologically related (one, two initial phonemes), semantically related (low, high relatedness), or unrelated.	High Phonological similarity (High_phon)	M = -0.008 ± 0.10	(Tyler et al., 2013)
				Range = (-0.3 – 0.3)	
				Missing = 4.3%	
			High semantic similarity (High_sem)	M = -0.04 ± 0.08	
				Range = (-0.35 – 0.25)	
				Missing = 4.3%	
			Low Phonological similarity (Low_phon)	M = 0.06 ± 0.08	
				Range = (-0.20 – 0.35)	
				Missing = 4.3%	
			Low semantic similarity (Low_sem)	M = 0.02 ± 0.09	
				Range = (-0.4 – 0.4)	

				Missing = 4.3%	
			Response time of High_phon in milliseconds (RT_high_phon)	M = -1.93 ± 95.13	
				Range = (-579 – 447)	
				Missing = 14.15%	
			Response time of High_sem in milliseconds (RT_high_sem)	M = 22.75 ± 87.7	
				Range = (-471 – 482)	
				Missing = 14.15%	
			Response time of Low_phon in milliseconds (RT_low_phon)	M = 47.74 ± 81.47	
				Range = (-342 – 404)	
				Missing = 14.15%	
			Response time of Low_sem in milliseconds (RT_low_sem)	M = 24.45 ± 80.18	
				Range = (-289 – 339)	
				Missing = 14.15%	
	Tip of Tongue	Participants name famous faces, indicate they don't know the name, or say "TOT" if they are having a tip of the tongue.	Tip of Tongue (ToT)	M = -0.47 ± 0.24	(Burke et al., 2004)
				Range = (-1 – 0.001)	
				Missing = 4.65%	

2.3 MRI data acquisition - The structural (T1, DWI) and functional data (rs-fMRI) were collected at a single site (MRC Cognition and Brain Sciences Unit) using 3 Tesla by CamCAN consortium in a Siemens scanner with a 32-channel head coil, where head movement was restricted with memory foam cushions. A high-resolution 3D structural T1-weighted image was acquired using the Magnetization-Prepared Rapid Gradient-Echo (MPRAGE) sequence with a Generalized Autocalibrating Partially Parallel Acquisition (GRAPPA) acceleration factor, repetition time (TR) = 2250 ms, echo time (TE) = 2.99 ms, inversion time (TI) = 900 ms, flip angle $\alpha = 9°$, field of view (FOV) = 256 × 240 × 192 mm, isotropic resolution = 1 mm, acquisition time of 4 min and 32 s. rs-fMRI scans were undertaken with echo planar imaging (EPI) sequences comprising of 261 volumes with eye-closed condition. Each volume consisted of 32 axial slices with slice thickness 3.7 mm, TR = 1,970 ms, TE = 30 ms, flip angle

$\alpha = 78°$, FOV = 192 × 192 mm^2, resolution = 3 × 3 × 4.44 mm acquired in descending order for 8 mins and 40 s.

Diffusion-weighted MR images (DWI) were obtained using a twice-refocused spin-echo (TRSE) echo-planar imaging sequence to reduce distortions caused by Eddy currents. The imaging scheme comprised 30 diffusion gradient directions for each of the two nonzero b-values (1,000 and 2,000 s/mm^2) and three images with zero b-values (0 s/mm^2). The other imaging parameters were as follows: 66 axial slices, isotropic resolution = 2 mm, TR/TE = 9100/104 ms, acquisition time = 10 min, and 2 s.

2.4 rs-fMRI preprocessing–Resting-state functional imaging data of each participant were preprocessed and denoised using the CONN toolbox version 2022a (https://www.nitrc.org/projects/conn ; Whitfield-Gabrieli & Nieto-Castanon, 2012) in conjunction with SPM12 and Matlab 2022a. The first five scans from each run were disregarded to allow the magnetization to reach a steady state (Caballero-Gaudes & Reynolds, 2017). Functional realignment was performed by the co-registration and resampling of all functional scans to a reference image using b-spline interpolation (Andersson et al., 2001). Temporal misalignment between different slices of functional data was corrected using a slice-timing correction (STC) procedure (Henson et al., 1999). Outlier detection was performed with the help of Artefact Detection Tool (ART, https://www.nitrc.org/projects/artifact_detect/), in which framewise displacement above 0.9 mm or global BOLD signal changes above 5 standard deviations were flagged as potential outliers and a new reference image was generated by averaging across all scans excluding the outliers. Subsequently, the functional and structural data were independently normalized into a standard MNI template and segmented into gray matter, white matter, and CSF using a unified segmentation and normalization method (Ashburner & Friston, 2005). The output data were resampled to a default 180 × 216 × 180 mm bounding box using fourth-order spline interpolation, with 2 mm and 1 mm isotropic voxels for functional and anatomical data, respectively.

2.5 Denoising – Physiological fluctuations have been proven to be a considerable contributor to the noise present in BOLD signals (Krüger & Glover, 2001; Liu et al., 2006). To mitigate this issue, an additional preprocessing step was implemented, which involves an anatomical component-based noise correction method (aCompCor ; Behzadi et al., 2007). This algorithm utilizes principal component analysis (PCA) to characterize signals of non-neural origin, such as white matter and cerebrospinal fluid (5 components from each), and then introduces them as covariates in a general linear model (GLM) as an estimate of the physiological noise signal space. Concurrently, 12 motion parameters

(three translations, three rotations, and their first-order derivatives) and a variable number of noise components from each identified outlier scan were also regressed from the BOLD signal of each voxel. A simultaneous band-pass filtering (.009 Hz – .08 Hz) was applied, using a discrete cosine transform operation, to prevent any frequency mismatch in the nuisance regression strategy (Hallquist et al., 2013). The use of the aCompCor method significantly improves the sensitivity and specificity of functional connectivity estimates; thus, global signal regression was not applied (Chai et al., 2012; Muschelli et al., 2014).

2.6 Language network (LAN) selection – To evaluate the variation in FC within a defined LAN across age, a functional connectivity analysis was carried out using a FreeSurfer-based atlas, Desikan Killiany (Desikan et al., 2006). This automatic parcellation, based on hemispheric-specific anatomical features, has been shown to show high accuracy compared to manual labelling (Desikan et al., 2006), and has also been used in various language-related studies (Nilakantan et al., 2017; Papanicolaou et al., 2017; Qi et al., 2019). With the purpose of investigating the canonical regions of the LAN, we selected parcels that were most strongly aligned with the language areas identified in previous research (Bolognini & Martin, 2023; Branco et al., 2020; Zhang et al., 2021). The language-related region of interests (ROIs) included temporal regions, namely the Middle Temporal Gyrus (MTG), Superior Temporal Gyrus (STG), and superior temporal sulcus (STS), and inferior frontal regions, namely Pars Opercularis (PrasO) and Pars Triangualris (ParsT). Note that these regions of the frontal lobe are also known in the Brodmann (BA)-based terminology as BA 44 and BA 45, making up the classical Broca's area.

2.7 Functional connectome – For evaluating the functional connectivity (FC) within LAN, mean regional BOLD time series were estimated for each individual LAN-ROI. FC between two distinct brain ROIs was determined by calculating the partial correlation coefficients between the respective mean regional BOLD time series, accounting for the signals in all other brain regions. This approach provides a more precise depiction of direct functional interactions (Marrelec et al., 2006) by eradicating the influence of common sources and results in sparser FC matrices, compared to the conventional Pearson correlation approach (Smith et al., 2011; Zalesky et al., 2012). To draw statistical comparisons, the resulting connectivity values were then normalized using Fisher's r-to-z transformation.

2.8 DWI preprocessing – We developed a custom shell script (GitHub link) to preprocess the DWI data, which included the use of different software packages: MRtrix3 (https://www.mrtrix.org/ ;

Tournier et al., 2019), FSL (https://fsl.fmrib.ox.ac.uk/fsl/fslwiki ; Smith et al., 2004; Woolrich et al., 2009), Freesurfer (https://surfer.nmr.mgh.harvard.edu/ ; Fischl, 2012), and ANTs (https://github.com/stnava ; Tustison et al., 2010). Primarily, DWI data were de-noised with the function *dwidenoise*, which relies on the theory of Marchenko-Pastur Principal Component Analysis (MP-PCA ; Veraart et al., 2016), and then Gibb's ringing artifacts were removed using the sub-voxel shift method (Kellner et al., 2016). Motion and distortion correction was applied using *dwifslpreproc* function which implements FSL integrated tools: *topup* tool was used for susceptibility-induced distortion correction (Andersson et al., 2003; S. M. Smith et al., 2004) and *eddy* for within-shell and between-shell motion and eddy current-induced distortion correction (Andersson et al., 2016). Bias field correction (Tustison et al., 2010) was applied using the MRtrix function *dwibiascorrect* with *the-ants* option to improve the brain mask estimation.

2.9 Fibre orientation distribution (FOD) – Initially, response functions for distinct tissue types (white matter, gray matter, and cerebrospinal fluid) were estimated using the *dwi2response* function with the Dhollander algorithm, which is specifically designed for multi-shell data (Dhollander et al., 2019). Subsequently, the orientation of fibres in each voxel was estimated using *dwi2fod* function with the multi-shell multi-tissue constrained spherical deconvolution (MSMT-CSD) algorithm (Jeurissen et al., 2014), which have demonstrated superior performance compared to diffusion tensor imaging (DTI) in regions with crossing-fibres (Farquharson et al., 2013; Tournier et al., 2008). Finally, to ensure the comparability of FODs across participants, global intensity normalization was conducted using the *mtnormalise* function.

2.10 Tractography – Anatomically Constrained Tractography (ACT) was applied to reduce false positives and improve the biological plausibility of streamline generation (Smith et al., 2012). To make the data suitable for ACT, each T1-weighted image was segmented into five tissue types (cortical gray matter, subcortical gray matter, white matter, cerebrospinal fluid, and pathological tissue) with FSL function *5ttgen* and then registered to the diffusion image with six degrees-of-freedom (DOF) using *flirt* tool from FSL (Greve & Fischl, 2009; Jenkinson et al., 2002). A streamline seeding mask was defined between the interface of white matter and gray matter using *the 5ttgmwmi* function. Hereafter, *the-act* and *-backtrack* options were adopted with *the tckgen* function to anatomically constrain the extent of streamline propagation and allow resampling of a streamline if it terminates in an unexpected location (e.g., cerebrospinal fluid). A probabilistic tractography algorithm was used, as it integrates FODs more accurately by considering second-order tensor information, leading to improved streamline propagation (Tournier et al., 2010). For each participant, 10 million tracts were generated with a

specified maximum tract length (250 mm) and cut-off FOD amplitude (0.06) from an iterative procedure with random placement of seeds within the mask. These tracts were further refined by using *tcksift2* function, which determines appropriate cross-sectional area multipliers for each streamline. This algorithm optimizes the streamline weights to ensure that the reconstructed fibre volumes correspond accurately with those estimated from the underlying diffusion signal, thereby providing a more reliable and accurate measure of fibre connectivity (Smith et al., 2015). Moreover, the tractograms were visually inspected to ensure comprehensive coverage of the white matter and to confirm that the streamlines were confined within the white matter boundaries.

2.11 Structural connectome – Each participant's anatomical image was initially segmented into distinct brain regions utilizing the same atlas employed during the functional connectivity analysis (Desikan et al., 2006), with *the recon-all* command (Fischl et al., 2004). The atlas-based parcellation image, along with streamline weights and tractography data, was then utilized to generate a symmetric connectivity matrix using the MRtrix function *tck2connectome* (Tournier et al., 2019). The resulting connectivity matrix was scaled with the inverse of node volumes, eliminating biases due to varying brain region sizes and facilitating more accurate and comparable measurements of connectivity strength across different regions (Hagmann et al., 2008). Inter-subject connection density normalization was achieved by adjusting the streamline weights with a proportionality coefficient, such that each matrix entry denotes the total intra-axonal cross-sectional area of the axons associated with the fiber bundle of interest, referred to as the fiber bundle capacity (FBC ; Smith et al., 2022).

2.12 Statistical modeling and testing – In this study, we implemented linear mixed-effects modeling (LME), a widely recognized and robust statistical framework for analyzing neuroimaging and behavioral data, particularly in studies involving repeated measures and hierarchical structures (G. Chen et al., 2013, 2014; Chua et al., 2015; Jones et al., 2013). This approach effectively controls for Type I errors while maintaining high statistical power (Galbraith et al., 2010; Riha et al., 2020; Scandola & Tidoni, 2021). Unlike traditional linear regression models, LME models account for both fixed effects (e.g., age, FC, and SC) and random effects (e.g., inter-subject variability in gender and education), making them particularly well-suited for the design of the current study.

For this analysis, we adopted a model comparison approach in which a full model (including all fixed and random effects) was compared to a null model (including all random effects, but excluding one fixed effect). To determine whether the inclusion of a specific fixed effect significantly improved the model fit, we performed an analysis of variance (ANOVA) to compare the two models, a method that

is well supported by previous research in cognitive neuroscience (Riha et al., 2020; Scandola & Tidoni, 2021). Additionally, model fit was further evaluated using the Akaike Information Criterion (AIC) and Bayesian Information Criterion (BIC), with lower values indicating a superior fit (Burnham & Anderson, 2002) and, hence, better predictability. To control for multiple comparisons in the post-hoc analysis, we applied the False Discovery Rate (FDR) correction, reducing the likelihood of Type I errors and ensuring the robustness of p-values (Benjamini & Hochberg, 1995).

All statistical analyses were performed in R version 4.4.1 (https://www.r-project.org/) using the lme4 (Bates et al., 2015) and lmerTest (Kuznetsova et al., 2017) packages. The lme4 package was used to fit all LMEs, while the lmerTest package was employed to provide significance tests for the fixed effects by incorporating Satterthwaite's approximation of degrees of freedom, ensuring more reliable p-values in the mixed-effects models. Graphical representations of the results were generated using the ggplot2 package (Wickham, 2016), version 3.5.1, and all the nodes and edges of the LAN were visualized thro ugh schematic brain plots created using BrainNet viewer (Xia et al., 2013).

2.12.1 Behaviour analysis - The behavioral scores for each of the 16 subdomains across the LC and production tasks were first standardized using z-score normalization in R, ensuring comparability across tasks. Missing data were handled on a task-specific basis by removing rows with missing values for each respective behavioral task, while preserving data for other tasks. Following data preprocessing, a model comparison approach was implemented for each language-behavior task. The full model, which included age as a fixed effect alongside random effects for gender and education (Equation 2), was compared with a null model that excluded age as a fixed effect (Equation 1). The comparison between these models allowed for the evaluation of age as a significant predictor of language behaviour. P-values from the ANOVA (comparing two models) were FDR-corrected to statistically compare the estimate of age across each language behavior task.

$$Language\ behaviour\ \sim\ 1\ +\ (1|gender) +\ (1|Education) \qquad (1)$$

$$Language\ behaviour\ \sim\ 1\ +\ age\ +\ (1|gender) +\ (1|Education) \qquad (2)$$

2.12.3 SC analysis – Prior to analysis, SC values from each of the edge within LAN were standardized using z-score normalization to mitigate potential bias in parameter estimation and enhance model convergence. To investigate age-related differences in intra-hemispheric and inter-hemispheric SCs, we applied an LME model similar to the approach described earlier. A full model (Equation 4),

incorporating age as a fixed effect while controlling for gender and education as random effects, was compared to a null model (Equation 3), which included only the random effects. The models were compared using ANOVA, with the resulting p-values subjected to FDR correction to account for multiple comparisons and minimize Type I errors.

$$SC \sim 1 + (1|gender) + (1|Education) \quad (3)$$

$$SC \sim 1 + age + (1|gender) + (1|Education) \quad (4)$$

2.12.2 FC analysis – Analogous to the SC analysis, normalized FC values for each of the 45 edges were employed to investigate age-related FC variations for all edges. The full model (Equation 6) was compared with the null model (Equation 5) to estimate the effect of age as a predictor of FC, with random effects for gender and education controlled in both models. Statistical comparisons between models were carried out using ANOVA, with FDR correction applied to the resulting p-values.

$$FC \sim 1 + (1|gender) + (1|Education) \quad (5)$$

$$FC \sim 1 + age + (1|gender) + (1|Education) \quad (6)$$

2.12.3 Interaction analysis – To assess the effect of brain connectivity (SC and FC) on the variation in brain behaviour (Language) across age, an initial analysis was conducted with the approach, using LME models. However, the model encountered convergence issues, likely due to the complexity of the data and the non-linear relationships between variables. A promising alternative for more flexible modeling is the Generalized Additive Mixed Model (GAMM; Lin & Zhang, 1999; Wood, 2017) because it does not require a priori knowledge of the functional form for modeling language behaviour specific trends with brain connectivity and its interaction with age. Specifically, GAMM substitute the fixed linear slopes with flexible 'smooth' functions to capture non-linear relationships and provide more robust estimates that can be applied to complex cross-sectional cognitive data (Roger et al., 2023; Sørensen, Brandmaier, et al., 2021).

In this study, GAMMs were implemented using *bam* function from *mgcv* package in the R library (version 1.9; Wood, 2017). Given that our primary objective was to explore how SC and FC influence language abilities/ behavior (LB) as a function of age, we adopted an interaction-based modeling approach to capture the dynamic interplay between connectivity and behavior across age. This

approach utilized tensor-product smooth functions ($te()$) to capture the combined influence of age and brain connectivity measures, while random effects, such as gender and education, were accounted for using smooth terms ($s()$). The final models used in the analysis were as follows:

$$LB \sim 1 + te(SC, age) + s\ (RE) \quad (7)$$

$$LB \sim 1 + te(FC, age) + s\ (RE) \quad (8)$$

where, RE represents the random effects such as gender, education. Other than the main effects, we undertook post-hoc model comparisons using ANOVA, where each interaction model (Equations 7–8) was compared to a baseline age-only model

$$LB \sim 1 + s(age) + s(RE) \quad (9)$$

This allowed us to evaluate whether including connectivity as an interaction term significantly improved model fit in explaining variations in LB. Finally, the predictor matrix derived from the GAMM (equation 7, 8) was employed to derive non-linear trajectories of the interaction term, which significantly modelled the variability in language behavior.

3. Results

3.1 Variation of performance in language comprehension (LC) and production (LP) tasks across lifespan

To explore the impact of age on performance across the 16 subdomains of LC and LP tasks, the age estimates from full LME (Equation 2) were plotted with their respective error bars (Figure 1C). As anticipated, vocabulary (vocab) and proverb comprehension demonstrated the strongest positive associations with age, with significant estimates even after adjusting the p-values for multiple comparisons (Vocab: $\beta = 0.017$, FDR-corrected $p < 0.0001$; Proverb: $\beta = 0.012$, FDR-corrected $p < 0.0001$). However, LP tasks, including Verbal Fluency (VF), five subdomains of the picture priming (RT_low_phon, RT_low_sem, RT_high_phon, RT_high_sem, and High_sem), and the tip-of-the-tongue (ToT), demonstrated significant decline in performance with age (Figure 1C; VF: $\beta = -0.012$, FDR-corrected $p < 0.001$; RT_low_phon: $\beta = -0.009$, FDR-corrected $p < 0.001$; RT_low_sem: : $\beta = -0.007$, FDR-corrected $p < 0.05$; RT_high_phon: $\beta = -0.006$, FDR-corrected $p < 0.05$; RT_high_sem: $\beta = -0.006$, FDR-corrected $p < 0.05$; High_sem: $\beta = -0.008$, FDR-corrected $p < 0.01$; ToT: $\beta = -0.016$, FDR-corrected $p < 0.001$). In contrast to the high semantic similarity condition (High_sem), no significant age-related changes were observed in the accuracy of the high phonological similarity condition in the picture priming task (High_phon: $\beta = -0.003$, FDR-corrected $p = 0.16$). Interestingly, performance among both accuracy and response time measures in the sentence comprehension tasks (Syn_comp, Sem_comp, RT_Syn_comp, and RT_Sem_comp) were not affected by age-related variation across the lifespan (Figure 1C; Syn_comp: $\beta = 0.001$, FDR-corrected $p = 0.58$; Sem_comp: $\beta = -0.0006$, FDR-corrected $p = 0.82$; RT_Syn_comp: $\beta = -0.003$, FDR-corrected $p = 0.26$; and RT_Sem_comp: $\beta = -0.001$, FDR-corrected $p = 0.81$).

3.2 Age-related variation in structure of language network (LAN)

The relationship between structural connectivity within the LAN and age was visualized using schematic brain plots and horizontal plots (Figure 2) based on the age-related beta coefficients from full LME model (Equation 4). Examination of intra-hemispheric structural connectivity patterns revealed significant age-related alterations in both cerebral hemispheres, encompassing both increases and decreases in connectivity. Interestingly, a greater number of left-hemispheric SCs showed significant negative association with age (Figure 2A; No. of connections = 6/10; FDR-corrected $p < 0.05$) as compared to the right-hemispheric SCs (Figure 2B; No. of connections = 3/10; FDR-corrected

$p < 0.05$). The connection strength within the right Broca's area (RParsO_RParsT) showed a significant increase with age ($\beta = 0.006$, FDR-corrected $p < 0.01$), whereas the SC between the left Pars-opercularis (LParsO) and left Pars-triangularis (LParsT) demonstrated a significant age-related decrease ($\beta = -0.005$, FDR-corrected $p < 0.05$). Additionally, most intra-hemispheric fronto-temporal connections displayed a general pattern of age-related decline, including connections between Broca's area and the superior temporal sulcus (LSTS_LParsO: $\beta = -0.012$, FDR-corrected $p < 0.001$, LSTS_LParsT: $\beta = -0.009$, FDR-corrected $p < 0.001$, and RSTS_RParsT: $\beta = -0.007$, FDR-corrected $p < 0.01$), as well as the middle temporal gyrus (LMTG_LParsO: $\beta = -0.021$, FDR-corrected $p < 0.001$, LMTG_LParsT: $\beta = -0.018$, FDR-corrected $p < 0.001$, RMTG_RParsO: $\beta = -0.01$, FDR-corrected $p < 0.001$, and RMTG_RParsT: $\beta = -0.016$, FDR-corrected $p < 0.001$). Contrary to this overall trend of age-related decline, the structural strength of intra-hemispheric temporo-temporal connections showed significant positive association with age, involving the STS, MTG, and STG among both hemispheres (LSTS_LMTG: $\beta = 0.019$, FDR-corrected $p < 0.001$, LSTS_LSTG: $\beta = 0.014$, FDR-corrected $p < 0.001$, LMTG_LSTG: $\beta = 0.014$, FDR-corrected $p < 0.001$, RSTS_RMTG: $\beta = 0.012$, FDR-corrected $p < 0.001$, RSTS_RSTG: $\beta = 0.016$, FDR-corrected $p < 0.001$, RMTG_RSTG: $\beta = 0.004$, FDR-corrected $p < 0.05$).

Regarding inter-hemispheric SCs, although a few connections remained stable across age (Figure 2C; No. of connections = 6/25: LMTG_RSTG: $\beta = -0.0003$, FDR-corrected $p = 0.89$, LMTG_RMTG: $\beta = -0.0003$, FDR-corrected $p = 0.16$, LSTG_RMTG: $\beta = 0.0046$, FDR-corrected $p = 0.059$, LSTS_RParsT: $\beta = -0.0016$, FDR-corrected $p = 0.56$, LParsT_RSTS: $\beta = -0.0035$, FDR-corrected $p = 0.11$, LParsT_RSTG: $\beta = -0.0039$, FDR-corrected $p = 0.10$), the majority showed significant age-related changes (Figure 2C; No. of connections = 19/25; FDR-corrected $p < 0.05$). Two primary patterns were readily observable among the notable age-related variations in the inter-hemispheric SCs. One of the trends consisted a significant decline in the SC of fronto-temporal (LParsO_RMTG: $\beta = -0.014$, FDR-corrected $p < 0.001$, LParsO_RSTG: $\beta = -0.012$, FDR-corrected $p < 0.001$, LParsO_RSTS: $\beta = -0.008$, FDR-corrected $p < 0.001$, LParsT_RMTG: $\beta = -0.006$, FDR-corrected $p < 0.05$, LMTG_RParsO: $\beta = -0.014$, FDR-corrected $p < 0.001$, LSTG_RParsO: $\beta = -0.008$, FDR-corrected $p < 0.001$, LMTG_RParsT: $\beta = -0.007$, FDR-corrected $p < 0.01$, LSTS_RParsO: $\beta = -0.006$, FDR-corrected $p < 0.05$, LSTG_RParsT: $\beta = -0.005$, FDR-corrected $p < 0.05$) and fronto-frontal connections (LParsO_RParsO: $\beta = -0.015$, FDR-corrected $p < 0.001$, LParsO_RParsT: $\beta = -0.014$, FDR-corrected $p < 0.001$, LParsT_RParsO: $\beta = -0.011$, FDR-corrected $p < 0.001$, LParsT_RParsT: $\beta = -0.006$, FDR-corrected $p < 0.05$). Conversely, the inter-hemispheric temporo-temporal showed significant strengthening with age, particularly between the left and right hemispheric regions of the STS, MTG,

and STG (LSTS_RTS: $\beta = 0.011$, FDR-corrected $p < 0.001$, LSTS_RMTG: $\beta = 0.008$, FDR-corrected $p < 0.001$, LSTS_RSTG: $\beta = 0.010$, FDR-corrected $p < 0.001$, LMTG_RSTS: $\beta = 0.005$, FDR-corrected $p < 0.05$, LSTG_RSTG: $\beta = 0.006$, FDR-corrected $p < 0.01$, and LSTG_RSTS: $\beta = 0.012$, FDR-corrected $p < 0.001$).

3.3 Age-related variation in functional connecvity among LAN nodes

The age estimates derived from the full LME model for FC (Equation 6) were utilized to investigate the edge-specific variation in functional connectivities within the LAN across the lifespan (Figure 3). LME modeling revealed distinct patterns of age-related changes in FC within the intra- and inter-hemispheric connections of the LAN. In the case of intra-hemispheric FCs, connections within the left hemisphere demonstrated both significant negative (Figure 3A; No. of connections = 3/10: LSTS–LMTG, LSTS–LSTG, and LParsO_LSTG; FDR-corrected $p < 0.05$) and positive (Figure 3A; No. of connections = 1/10: LMTG_LSTG; FDR-corrected $p < 0.05$) associations with age, whereas no significant age-related associations were found for right-hemispheric functional connections (Figure 3B; No. of connections = 0/10; FDR-corrected $p > 0.05$). Within left-hemispheric FCs, among temporo-temporal connections, FC associated with STS region showed significant decline with age (LSTS–LMTG: $\beta = -0.0039$, FDR-corrected $p < 0.001$; LSTS–LSTG: $\beta = -0.0023$, FDR-corrected $p < 0.01$), whereas FC between MTG and STG demonstrated a significant positive association with age ($\beta = 0.0023$, FDR-corrected $p < 0.01$). Considering inter-hemispheric FCs, most connections remained unaffected by age (Figure 3C; No. of connections = 24/25; FDR-corrected $p > 0.05$). However, a significant age-related decrease was observed in the FC between the left and right middle temporal gyri (MTG) ($\beta = -0.003$, FDR-corrected $p < 0.05$).

3.4 Non-linear relationship between edge-specific SC and age-related language variability

To examine the role of edge-specific SC in modulating the relationship between language behavior and age, a tensor product smooth term was incorporated into the GAMM model (Equation 7) independently for each of the 16 language behavior tasks and 45 SC edges. The results were visualized in a heatmap (Figure 4A) of estimated degrees of freedom (edf) values, while model performance metrics, including adjusted R^2, AIC, F-statistic, FDR-corrected p-values, and fREML, were summarized in Supplementary Table1. The edf values represent the degree of non-linearity in the relationship between SC and language behavior. Specifically, an edf value of 1 indicates a linear association, $1 < edf \leq 2$ indicates a weakly non-linear association, and $edf > 2$ indicates a highly non-linear relationship (Wood, 2017). In our case, the blue shades in the heatmap represent all significant interactions with edf values greater than 2, where deeper shades correspond to even higher EDF values, indicative of highly non-

linear relationships. The significant non-linear interactions (FDR-corrected $p < 0.05$) were predominantly observed in LP tasks (Figure 4A; e.g., picture priming, VF, and ToT), with some cases observed in comprehension tasks (Figure 4A; e.g., Vocab and Proverb). Specifically, performance in the VF, ToT, Vocab, and proverb tasks demonstrated significant age-related SC modulation (FDR-corrected $p < 0.001$) across both intra- and inter-hemispheric edges (Figure 4A; 45 of 45 SC edges). In the Picture Priming task, age-related variations in tasks with low phonological and semantic demands were significantly associated (FDR-corrected $p < 0.05$) with a greater number of LAN SC edges (e.g., Low_phon: 45 of 45 SC edges, RT_low_phon: 45 of 45 SC edges, and RT_low_sem: 35 of 45 SC edges) than tasks with higher phonological and semantic demands (e.g., High_phon: 0 of 45 SC edges, RT_high_phon: 0 of 45 SC edges, and RT_high_sem: 5 of 45 SC edges). While response time and accuracy in the Syn-Sem tasks showed no significant association (FDR-corrected $p > 0.05$) with age-related SC variations (Figure 4A), syntactically complex sentences (Syn_comp) emerged as an exception, with performance being significantly modulated by changes in specific SC edges (LMTG_RParsT: edf = 12.85, FDR-corrected $p < 0.001$, LParsT_LSTG: edf = 10.78, FDR-corrected $p < 0.05$, LSTG_RParsT: edf = 7.61, FDR-corrected $p < 0.001$, and LSTS_RParsT: edf = 5.62, FDR-corrected $p < 0.001$).The observed pattern of interactions modulating specific language behaviours closely mirrored the findings of the LME model (Equation 2), which assessed language behavior as a function of age alone. To validate these findings and ensure a consistent analytical approach, we also examined the non-linear relationship between language behavior and age only using GAMM (Equation 9). The results, visualized in Supplementary Figure 1, showed considerable overlap with those of the SC × age model, suggesting that age-related influences may have been a primary driver of these effects. To distinguish true interaction effects devoid of potential age-related artifacts, we conducted a post-hoc ANOVA to compare the full interaction model (Equation 7) with the baseline age-only model (Equation 9). The statistical significance of the interaction term was assessed, and the resulting F-values were visualized in a heatmap (Figure 4C), only a subset of SC × age interactions remained statistically robust (FDR-corrected $p < 0.05$) after accounting for general age-related influences. Among these, age-related structural changes in interhemispheric and left-hemispheric fronto-temporal connections were significantly associated with variations in language comprehension (e.g., Vocab: LMTG_RSTS, edf = 6.95, F = 5.04, FDR-corrected $p < 0.05$), particularly the comprehension of syntactically complex sentences (e.g., Syn_comp: LParsT_LSTG, edf = 10.78, F = 2.93, FDR-corrected $p < 0.01$; LSTS_RParsT, edf = 5.62, F = 13.77, FDR-corrected $p < 0.001$; LMTG_RParsT, edf = 12.85, F = 8.23, FDR-corrected $p < 0.001$; and LSTG_RParsT, edf = 7.61, F = 10.35, FDR-corrected $p < 0.001$). In contrast, age-related variation in reaction time of picture priming task high semantic similarity condition (RT_high_sem) was significantly associated with structural strength of

temporo-temporal connections, spanning both interhemispheric (LSTS_RSTS: edf = 6.09, F = 3.61, FDR-corrected $p < 0.01$; LSTS_RMTG: edf = 7.53, F = 2.76, FDR-corrected $p < 0.05$) and right-hemispheric pathways (RSTS_RSTG: edf = 7.39, F = 3.70, FDR-corrected $p < 0.01$). Additionally, accuracy in the same task (High_sem) was significantly modulated by structural strength of fronto-frontal inter-hemispheric connection (LParsT_RParsT, edf = 3.00, F = 35.98, FDR-corrected $p < 0.05$).

The significant interactions identified through ANOVA were further explored using GAMM trajectory plots (Figure 5A, 5B), where predicted behavioral trajectories were plotted across age for three SC quantiles (0.25, 0.50, and 0.75), highlighting differential effects of SC on language performance across the lifespan. Our findings revealed a differential role of SC in modulating age-related trajectories of LC and LP tasks, where SC influenced comprehension performance (Figure 5A) consistently across all ages (18-88 years), while its effect on production tasks (Figure 5B) became evident only in late adulthood (60–80 years). In comprehension tasks (Syn_comp, Vocab), higher SC among all significant edges was associated with better performance particularly at older age (Figure 5A). Whereas at younger age, SC exhibited differential effect, some edges supported the comprehension (LMTG_RParsT, LParsT_LSTG) while other edges (LSTG_RParsT, LSTS_ RParsT, LMTG_RSTS) displayed negative association with performance. However, for production tasks (High_sem, RT_high_sem), SC effects emerged only in older adults (70-88) with lower SC (LSTS_RMTG, LSTS_RSTS) was associated with better performance (Figure 5B).

3.5 Non-linear relationship between edge-specific FC and age-related language variability

This study investigated the role of intra- and inter-hemispheric FCs in non-linear modulation of language performance across age with the help of an interaction term (FC × age) that was incorporated in the GAMM model (Equation 8). The corresponding edf values for each model were visualized in a heatmap (Figure 4B) and all model performance-related parameters were documented in Supplementary table 3. Age-related variation in performance of LP tasks (VF, ToT, and Picture priming) across age were significantly modulated (FDR-corrected $p < 0.001$) by both intra- and inter-hemispheric FCs (Figure 4B; 45 of 45 FC edges). Notably, within the picture priming task, tasks characterized by low phonological and semantic similarity were significantly associated (FDR-corrected $p < 0.05$) with a greater number of LAN FC edges (Figure 4B; e.g., Low_phon: 40 of 45 FC edges, RT_low_phon: 45 of 45 FC edges, and RT_low_sem: 10 of 45 FC edges) than tasks with higher phonological and semantic similarity (Figure 4B; e.g., High_phon: 0 of 45 FC edges, RT_high_phon: 0 of 45 FC edges, RT_high_sem: 6 of 45 FC edges). In contrast, among LC tasks, only vocabulary and proverb comprehension demonstrated significant non-linear associations (Figure 4B; FDR-corrected p

< 0.001) with age-related FC changes within the LAN. Comprehension of syntactically complex sentences was unaffected by the influence of either intra- or inter-hemispheric FCs within the LAN (Figure 4B; FDR-corrected p > 0.05). However, age-related variation in comprehension ability of semantically complex sentences (Sem_comp) showed significant association with only two specific inter-hemispheric FCs (Figure 4B; LParsT_RParsO: edf = 6.41, FDR-corrected p <0.05; LParsO_RSTG: edf = 8.70, FDR-corrected p < 0.001).

The modulatory effects of FC × age on language behavior exhibited a pattern consistent with the LME model results (Equation 2). Similar to the SC × age interaction effects, a post-hoc ANOVA was conducted to compare the full FC × age model (Equation 8) with the baseline age-only GAMM model (Equation 9) to account for potential age-related confounds. This analysis allowed us to isolate the unique contribution of functional connectivity beyond age-related effects. The resulting F-values were visualized in a heatmap (Figure 4D), highlight the differential impact of interaction term on LC and LP tasks, where a greater number of production tasks (4 of 10 tasks: VF, High_sem, RT_low_sem, RT_low_phon) showed significant association (FDR-corrected p < 0.05) with interaction term than comprehension tasks (1 of 6 tasks: Sem_comp). In LC tasks, only interhemispheric FCs significantly contributed to age-related variations in the comprehension of semantically complex sentences (Figure 4D; LParsT_RParsO: edf = 6.41, F = 3.29, FDR-corrected p < 0.05; LParsO_RSTG: edf = 8.70, F = 5.23, FDR-corrected p < 0.001). In contrast, production tasks (VF, High_sem, RT_low_sem, RT_low_phon) engaged a broader FC network, including right-hemispheric (RT_low_sem: RMTG_RSTG, edf = 6.43, F = 3.35, FDR-corrected p < 0.05), left-hemispheric (High_sem: LMTG_LParsO, edf = 3.00, F = 6.25, FDR-corrected p < 0.05; LParsT_LSTG edf = 3.00, F = 16.24, FDR-corrected p < 0.05), and interhemispheric (High_sem: LParsO_RSTG, edf = 3.00, F = 4.75, FDR-corrected p < 0.05; High_sem: LSTG_RParsO, edf = 4.43, F = 30.14, FDR-corrected p < 0.05; RT_low_sem: LParsO_RParsO, edf = 7.83, F = 3.32, FDR-corrected p < 0.05; RT_low_phon: LParsO_RParsT, edf = 3.31, F = 13.00, FDR-corrected p < 0.01) connections.

To further explore the non-linear trajectories of these significant interaction effects, we examined GAMM trajectory plots (Figure 5C, 5D), where each FC quantile was represented by a distinct colour. These findings underscore the differential age-related modulation of LC (Figure 5C) and LP (Figure 5D) tasks by each specific FC edge. For comprehension tasks (Sem_comp), lower interhemispheric fronto-temporal FC (LParsO_RSTG) was associated with higher performance across the lifespan (Figure 5C), whereas the effect of interhemispheric fronto-frontal FC (LParsT_RParsO) reversed after middle age (60–70 years). For production tasks, the picture-priming task with high-semantic similarity (High_sem) displayed a consistent modulation pattern across all four FC edges (Figure 5D);

LParsO_RSTG, LSTG_RParsO, LMTG_LParsO, LParsT_LSTG), where the effects of higher and lower FC reversed near middle age (40–55 years). However, for the reaction time of picture-priming task with low-semantic and low-phonological similarity (RT_low_sem, RT_low_phon), the differential effect of lower and higher FC emerged only in older adults (70-88). Additionally, performance in the verbal fluency task (VF) was associated with higher interhemispheric FC (LParsO_RParsO) exclusively in younger adults (18–40 years), highlighting a unique early-life dependency on FC for verbal fluency processing.

4. Discussion

Cognitive aging is associated with an intriguing dichotomy in language abilities: LC is preserved or enhanced, whereas LP declines along lifespan(Burke & Shafto, 2004; Shafto & Tyler, 2014). Previous studies, often limited to a single modality (rsFC or SC) or linear models (Davis et al., 2009; Ferré et al., 2019; Fletcher et al., 2018; Gertel et al., 2020), have primarily reported increase in functional connectivity with aging in tandem with white matter loss and cortical thinning, giving rise to conflicting theories of compensation via specialized networks that serve as cognitive reserve (Cabeza et al., 2018) and contrarily, through reduction in specialized processing, also referred to as de-differentiation (Zhang & Diaz, 2023a). In this study, we integrated rsFC, SC, and behavioral data across a large lifespan sample, using a non-linear mixed model approach (GAMM) to capture subtle brain-behavior interactions. Consistent with prior findings, LP declined significantly with age, whereas LC remained stable or improved (Figure 1C). Structurally, we observed a decline in fronto-temporal and within-frontal connections, alongside strengthening within temporal lobe connections (Figure 2). Functionally, language network connectivity was largely preserved, with limited left- and interhemispheric decline (Figure 3). GAMM analyses suggest that neurocognitive aging is not a uniform process but reflects strategic network adaptations with differentially modulating comprehension versus production abilities across lifespan (Figure 4, 5). These findings underscore the importance of integrating functional and structural measures to understand the neural mechanisms underlying LC preservation and LP decline across lifespan.

Dichotomy in language abilities across age

Aligning with previous research (Burke & Shafto, 2004; Diaz et al., 2016; Ferré et al., 2019; Salthouse, 2014), our study revealed a striking dichotomy of age-related changes in language abilities, highlighting the decline of LP and preservation of LC across the lifespan (Figure 1C). Extending prior work, multiple tasks within each language category (LC and LP) were analyzed to provide a comprehensive profile of variations in language abilities across the adult lifespan. Among LP tasks, VF, picture priming and Tip of tongue (ToT) demonstrated a significantly reduced accuracy and prolonged response times with advancing age. These decline may be driven by weakened connections between semantic and phonological representations, reduced inhibitory control, and slower processing speeds, which collectively impair efficient lexical retrieval (Baciu et al., 2021; Diaz et al., 2014, 2016; Shafto et al., 2007). In contrast, performance in LC tasks were either preserved (sentence comprehension) or enhanced with age (vocabulary and proverb comprehension). This also aligns with the cognitive reserve hypothesis, which suggests that accumulated knowledge and experience can compensate for age-related neural decline (Cabeza et al., 2018).

Frontal vulnerability and temporal resilience

Intra-hemispheric SC exhibited more age-related declines in the left hemisphere compared to the right (Figure 2), consistent with previous reports of left-lateralized atrophy in older adults (Jao et al., 2020) and possibly explaining increased right-hemispheric activation during language comprehension (Geva et al., 2012; Peelle et al., 2010, 2013; Tyler et al., 2010). Fronto-temporal connections exhibited age-related bilateral SC reductions, particularly involving Broca's area (pars opercularis and triangularis) and temporal regions (STG, MTG, STS). Left-hemispheric fronto-frontal connections (LParsO-LParsT) also demonstrated age-related SC decline, aligning with "The frontal aging" hypothesis (Greenwood, 2000), which suggests that the frontal regions may be more susceptible to age-related degeneration. The frontal decline aligned with diffusion MRI evidence of reduced FA values and frontal atrophy in older adults (Jao et al., 2020; Madden et al., 2012; Pfefferbaum et al., 2005a). Conversely, SC within temporal regions were relatively preserved or strengthened, consistent with minimal FA changes and increased intra-temporal connectivity among older adults (Jao et al., 2020; Pfefferbaum et al., 2005b; Salat et al., 2005). Furthermore, the average strength of the right temporal module increased with age (Madden et al., 2020), supporting the anterior-posterior gradient of white matter decline (Sullivan et al., 2010), and the "last-in-first-out" model (Jao et al., 2020; Madden et al., 2012; Salat et al., 2005; Yang et al., 2014).

In contrast, inter-hemispheric SCs showed age-related decline in fronto-frontal and fronto-temporal connections, while temporal-temporal connections were preserved or enhanced. Such reorganization aligns with widely recognized pattern of anterior-to-posterior degeneration of corpus callosum (Bastin et al., 2010; Hou & Pakkenberg, 2012; Kochunov et al., 2007; Salat et al., 2005; Sullivan et al., 2010). Given that the anterior corpus callosum supports fronto-frontal and fronto-temporal connectivity, and the posterior corpus callosum connects bilateral temporal lobes (De Benedictis et al., 2016; Goldstein et al., 2025; Huang et al., 2005; Wang et al., 2020). The findings collectively highlight a dual trajectory of age-related neural reorganization: vulnerable frontal connections showing progressive decline contrasted with stable posterior-temporal integration.

FC compensates SC degradation

In contrast to SC, FC demonstrated a relative age-related resilience among LAN regions (Figure 3). However, selective decline were observed primarily in left- and inter-hemispheric connections, with significant age-related decreases in FC between LSTS-LSTG, LSTS-LMTG, and LParsO-LSTG, and an increase between LMTG and LSTG. The increased FC may be supported by enhanced SC between left temporal regions observed in this study. Similar to SC findings, FC aging showed an asymmetrical

trajectory, with significant reorganization in the left hemisphere and minimal changes in the right, suggesting right-hemispheric resilience, consistent with findings by Rafiq et al., (2022). The inter-hemispheric FC demonstrated age-related stability, with few observed age-related reorganizations (Figure 3C). Specifically, preservation of fronto-temporal FC despite SC decline may reflect compensatory mechanisms maintaining functional integrity across lifespan. Pistono et al., (2021) also observed that age-related FC is maintained despite of gray matter loss which is being followed up by our study.

Differential non-linear relationships of LC/LP with brain connectivity (FC/SC) across lifespan

GAMM analysis revealed significant non-linear associations between SC/FC and language behavior across the adult lifespan, undetected by linear approaches (Bolognini & Martin, 2023; Ferré et al., 2019), consistent with prior work validating GAMMs for lifespan modelling (Sørensen et al., 2021). Initial GAMM analysis (Equation 7,8) showed widespread interaction effects across language tasks (Figure 4 A,B), and subsequent ANOVA comparisons isolated interactions robust to general age-related effects (Figure 4 C,D). Trajectory plots (Figure 5) revealed a differential modulation of LC and LP tasks by SC/FC quantiles (0.25, 0.50, 0.75), characterized by distinct non-linear patterns across specific edges.

SC × age interactions within LC tasks were prominent in both intra- and interhemispheric fronto-temporal pathways, particularly affecting syntactic comprehension and vocabulary. Syn_comp was modulated by left-hemispheric and interhemispheric fronto-temporal SCs (LParsT_LSTG, LMTG_RParsT, LSTG_RParsT, LSTS_RParsT), consistent with the critical role of left fronto-temporal regions in syntax (Den Ouden et al., 2019; Price, 2010; Wilson et al., 2011) and bilateral reorganization with aging (Tyler et al., 2010). Lesion studies further implicate posterior callosal regions in syntactic comprehension deficits (Friederici, 2011; Friederici et al., 2007). Increased interhemispheric fronto-temporal SC (LSTG_RParsT, LSTS_RParsT) was associated with better syntactic comprehension in older adults, suggesting compensatory bilateral structural engagement. In contrast, Vocab performance in younger adults was negatively associated with interhemispheric SC (LMTG_RSTS), indicating that increased SC can be maladaptive depending on age and task demands. For LP tasks, only high semantic priming (High_sem) showed significant SC × age interaction, with distinct SC modulation emerging in older adults (70–88 years). High_sem task accuracy involved only interhemispheric fronto-frontal connection (LParsT_RParsT), while response time (RT_high_sem) involved both inter- and intra-hemispheric temporo-temporal connections (LSTS_RMTG, LSTS_RSTS, RSTS_RSTG). Prior studies (Chen et al., 2021) found no significant white matter effects

on response time or accuracy under semantic priming, likely due to linear model limitations, and others (Baldo et al., 2013; Jarret et al., 2022) focused only on the left hemisphere. Our findings highlight a dominant trend in older adults, where increased interhemispheric SC (LSTS_RMTG, LSTS_RSTS, LParsT_RParsT) did not improve performance, suggesting maladaptive reorganization (Naeser et al., 2011) or a compensatory ceiling (Reuter-Lorenz & Cappell, 2008). Overall, the differential non-linear effects of SC on language comprehension and production tasks across the lifespan suggest that SC plays a more nuanced role, with both compensatory and maladaptive mechanisms emerging depending on age and specific language task demands.

FC × age interactions within LC tasks were limited to semantically complex sentence comprehension (Sem_comp), modulated by interhemispheric fronto-temporal (LParsO–RSTG) and fronto-frontal (LParsT_RParsO) connections. Lower fronto-temporal FC was associated with better performance across ages, suggesting reduced interhemispheric interference benefits semantic processing, whereas higher fronto-frontal FC supported performance in older adults, consistent with compensatory recruitment under the CRUNCH model (Reuter-Lorenz & Cappell, 2008). Within LP tasks (Figure 5D), FC showed age-dependent modulation across both picture-priming (High_sem, RT_low_sem, RT_low_phon) and verbal fluency (VF) tasks. VF performance followed an inverted-U shaped trajectory associated with interhemispheric fronto-frontal FC (LParsO_RParsO), aligning with cognitive flexibility patterns (Uddin, 2021). Picture-priming tasks showed edge-specific modulation by intra- and inter-hemispheric FC, where enhanced left-lateralized and interhemispheric fronto-frontal FC (LParsO_RSTG, LSTG_RParsO, LMTG_LParsO, LParsT_LSTG) supported better semantic processing in older adults, again consistent with compensatory models (Reuter-Lorenz & Cappell, 2008).

This study elucidates that differential language aging arises from a dynamic interplay between structural vulnerability-particularly in frontal regions-and compensatory functional reorganization, notably within temporal and interhemispheric connections. Using a large, representative cohort, we identified “frontal vulnerability” and “temporal resilience” as key neuroanatomical signatures, supporting anterior-to-posterior and last-in-first-out models of white matter aging (Bastin et al., 2010; Madden et al., 2020; Salat et al., 2005; Sullivan et al., 2010). These mechanisms underlie preserved comprehension and declining production, with compensatory strategies aligning with the CRUNCH model (Reuter-Lorenz & Cappell, 2008). Clinically, our findings suggest that targeting temporal lobe connectivity may help mitigate language decline and delay symptoms in neurodegenerative disorders (Mascali et al., 2018; Rafiq et al., 2022; Rahul & Joseph Ponniah, 2019). Longitudinal and intervention

studies are needed to further elucidate the dynamic relationship between brain connectivity and language performance in aging.

Data and Code availability:

The neuroimaging data of cognitively healthy participants were obtained from CamCAN repository (available at CamCAN Data Repository; Shafto et al., 2014; Taylor et al., 2017). Custom shell script developed for DWI preprocessing can be downloaded from GitHub (GitHub Repository)

References

Andersson, J. L. R., Graham, M. S., Zsoldos, E., & Sotiropoulos, S. N. (2016). Incorporating outlier detection and replacement into a non-parametric framework for movement and distortion correction of diffusion MR images. *NeuroImage*, *141*, 556–572. https://doi.org/10.1016/j.neuroimage.2016.06.058

Andersson, J. L. R., Hutton, C., Ashburner, J., Turner, R., & Friston, K. (2001). Modeling Geometric Deformations in EPI Time Series. *NeuroImage*, *13*(5), 903–919. https://doi.org/10.1006/nimg.2001.0746

Andersson, J. L. R., Skare, S., & Ashburner, J. (2003). How to correct susceptibility distortions in spin-echo echo-planar images: Application to diffusion tensor imaging. *NeuroImage*, *20*(2), 870–888. https://doi.org/10.1016/S1053-8119(03)00336-7

Ashburner, J., & Friston, K. J. (2005). Unified segmentation. *NeuroImage*, *26*(3), 839–851. https://doi.org/10.1016/j.neuroimage.2005.02.018

Baciu, M., Banjac, S., Roger, E., Haldin, C., Perrone-Bertolotti, M., Lœvenbruck, H., & Démonet, J.-F. (2021). Strategies and cognitive reserve to preserve lexical production in aging. *GeroScience*, *43*(4), 1725–1765. https://doi.org/10.1007/s11357-021-00367-5

Baldo, J. V., Arévalo, A., Patterson, J. P., & Dronkers, N. F. (2013). Grey and white matter correlates of picture naming: Evidence from a voxel-based lesion analysis of the Boston Naming Test. *Cortex; a Journal Devoted to the Study of the Nervous System and Behavior*, *49*(3), 658–667. https://doi.org/10.1016/j.cortex.2012.03.001

Bastin, M. E., Maniega, S. M., Ferguson, K. J., Brown, L. J., Wardlaw, J. M., MacLullich, A. M. J., & Clayden, J. D. (2010). Quantifying the effects of normal ageing on white matter structure using unsupervised tract shape modelling. *NeuroImage*, *51*(1), 1–10. https://doi.org/10.1016/j.neuroimage.2010.02.036

Bates, D., Mächler, M., Bolker, B., & Walker, S. (2015). Fitting Linear Mixed-Effects Models Using lme4. *Journal of Statistical Software*, *67*, 1–48. https://doi.org/10.18637/jss.v067.i01

Behzadi, Y., Restom, K., Liau, J., & Liu, T. T. (2007). A component based noise correction method (CompCor) for BOLD and perfusion based fMRI. *NeuroImage*, *37*(1), 90–101. https://doi.org/10.1016/j.neuroimage.2007.04.042

Benjamini, Y., & Hochberg, Y. (1995). Controlling the False Discovery Rate: A Practical and Powerful Approach to Multiple Testing. *Journal of the Royal Statistical Society: Series B (Methodological)*, *57*(1), 289–300. https://doi.org/10.1111/j.2517-6161.1995.tb02031.x

Bolognini, M., & Martin, D. C. (2023). *Characterization of age-related changes in sentence processing abilities and the resting-state language network.* PsyArXiv. https://doi.org/10.31234/osf.io/x85ak

Bosticardo, S., Schiavi, S., Schaedelin, S., Battocchio, M., Barakovic, M., Lu, P.-J., Weigel, M., Melie-Garcia, L., Granziera, C., & Daducci, A. (2024). Evaluation of tractography-based myelin-weighted connectivity across the lifespan. *Frontiers in Neuroscience*, *17*. https://doi.org/10.3389/fnins.2023.1228952

Branco, P., Seixas, D., & Castro, S. L. (2020). Mapping language with resting-state functional magnetic resonance imaging: A study on the functional profile of the language network. *Human Brain Mapping*, *41*(2), 545–560. https://doi.org/10.1002/hbm.24821

Burke, D. M., & Shafto, M. A. (2004). Aging and Language Production. *Current Directions in Psychological Science*, *13*(1), 21–24. https://doi.org/10.1111/j.0963-7214.2004.01301006.x

Burnham, K. P., & Anderson, D. R. (2002). *Model selection and multimodel inference: A practical information-theoretic approach* (2nd ed). Springer. http://site.ebrary.com/id/10047705

Caballero-Gaudes, C., & Reynolds, R. C. (2017). Methods for cleaning the BOLD fMRI signal. *NeuroImage*, *154*, 128–149. https://doi.org/10.1016/j.neuroimage.2016.12.018

Cabeza, R., Albert, M., Belleville, S., Craik, F. I. M., Duarte, A., Grady, C. L., Lindenberger, U., Nyberg, L., Park, D. C., Reuter-Lorenz, P. A., Rugg, M. D., Steffener, J., & Rajah, M. N. (2018). Maintenance, reserve and compensation: The cognitive neuroscience of healthy ageing. *Nature Reviews Neuroscience*, *19*(11), 701–710. https://doi.org/10.1038/s41583-018-0068-2

Chai, X. J., Castañón, A. N., Öngür, D., & Whitfield-Gabrieli, S. (2012). Anticorrelations in resting state networks without global signal regression. *NeuroImage*, *59*(2), 1420–1428. https://doi.org/10.1016/j.neuroimage.2011.08.048

Chan, M. Y., Alhazmi, F. H., Park, D. C., Savalia, N. K., & Wig, G. S. (2017). Resting-State Network Topology Differentiates Task Signals across the Adult Life Span. *The Journal of Neuroscience*, *37*(10), 2734–2745. https://doi.org/10.1523/JNEUROSCI.2406-16.2017

Chen, G., Adleman, N. E., Saad, Z. S., Leibenluft, E., & Cox, R. W. (2014). Applications of multivariate modeling to neuroimaging group analysis: A comprehensive alternative to univariate general linear model. *NeuroImage*, *99*, 571–588. https://doi.org/10.1016/j.neuroimage.2014.06.027

Chen, G., Saad, Z. S., Britton, J. C., Pine, D. S., & Cox, R. W. (2013). Linear mixed-effects modeling approach to FMRI group analysis. *NeuroImage*, *73*, 176–190. https://doi.org/10.1016/j.neuroimage.2013.01.047

Chen, P.-Y., Chen, C.-L., Tseng, H.-M., Hsu, Y.-C., Huang, C.-W. C., Chan, W. P., & Tseng, W.-Y. I. (2021). Differential Associations of White Matter Brain Age With Language-Related Mechanisms in Word-Finding Ability Across the Adult Lifespan. *Frontiers in Aging Neuroscience*, *13*. https://doi.org/10.3389/fnagi.2021.701565

Chua, A. S., Egorova, S., Anderson, M. C., Polgar-Turcsanyi, M., Chitnis, T., Weiner, H. L., Guttmann, C. R. G., Bakshi, R., & Healy, B. C. (2015). Handling changes in MRI acquisition

parameters in modeling whole brain lesion volume and atrophy data in multiple sclerosis subjects: Comparison of linear mixed-effect models. *NeuroImage: Clinical*, *8*, 606–610. https://doi.org/10.1016/j.nicl.2015.06.009

Cole, M. W., Bassett, D. S., Power, J. D., Braver, T. S., & Petersen, S. E. (2014). Intrinsic and task-evoked network architectures of the human brain. *Neuron*, *83*(1), 238–251. https://doi.org/10.1016/j.neuron.2014.05.014

Damoiseaux, J. S. (2017). Effects of aging on functional and structural brain connectivity. *NeuroImage*, *160*, 32–40. https://doi.org/10.1016/j.neuroimage.2017.01.077

Davis, S. W., Dennis, N. A., Buchler, N. G., White, L. E., Madden, D. J., & Cabeza, R. (2009). Assessing the effects of age on long white matter tracts using diffusion tensor tractography. *NeuroImage*, *46*(2), 530–541. https://doi.org/10.1016/j.neuroimage.2009.01.068

Davis, S. W., Dennis, N. A., Daselaar, S. M., Fleck, M. S., & Cabeza, R. (2008). Qué PASA? The Posterior-Anterior Shift in Aging. *Cerebral Cortex (New York, N.Y. : 1991)*, *18*(5), 1201–1209. https://doi.org/10.1093/cercor/bhm155

De Benedictis, A., Petit, L., Descoteaux, M., Marras, C. E., Barbareschi, M., Corsini, F., Dallabona, M., Chioffi, F., & Sarubbo, S. (2016). New insights in the homotopic and heterotopic connectivity of the frontal portion of the human corpus callosum revealed by microdissection and diffusion tractography. *Human Brain Mapping*, *37*(12), 4718–4735. https://doi.org/10.1002/hbm.23339

Den Ouden, D., Malyutina, S., Basilakos, A., Bonilha, L., Gleichgerrcht, E., Yourganov, G., Hillis, A. E., Hickok, G., Rorden, C., & Fridriksson, J. (2019). Cortical and structural-connectivity damage correlated with impaired syntactic processing in aphasia. *Human Brain Mapping*, *40*(7), 2153–2173. https://doi.org/10.1002/hbm.24514

Desikan, R. S., Ségonne, F., Fischl, B., Quinn, B. T., Dickerson, B. C., Blacker, D., Buckner, R. L., Dale, A. M., Maguire, R. P., Hyman, B. T., Albert, M. S., & Killiany, R. J. (2006). An automated labeling system for subdividing the human cerebral cortex on MRI scans into gyral based regions of interest. *NeuroImage*, *31*(3), 968–980. https://doi.org/10.1016/j.neuroimage.2006.01.021

Diaz, M. T., Johnson, M. A., Burke, D. M., & Madden, D. J. (2014). Age-related differences in the neural bases of phonological and semantic processes. *Journal of Cognitive Neuroscience*, *26*(12), 2798–2811. https://doi.org/10.1162/jocn_a_00665

Diaz, M. T., Rizio, A. A., & Zhuang, J. (2016). The Neural Language Systems That Support Healthy Aging: Integrating Function, Structure, and Behavior. *Language and Linguistics Compass*, *10*(7), 314–334. https://doi.org/10.1111/lnc3.12199

Farquharson, S., Tournier, J.-D., Calamante, F., Fabinyi, G., Schneider-Kolsky, M., Jackson, G. D., & Connelly, A. (2013). White matter fiber tractography: Why we need to move beyond DTI. *Journal of Neurosurgery*, *118*(6), 1367–1377. https://doi.org/10.3171/2013.2.JNS121294

Ferré, P., Benhajali, Y., Steffener, J., Stern, Y., Joanette, Y., & Bellec, P. (2019). Resting-state and vocabulary tasks distinctively inform on age-related differences in the functional brain connectome. *Language, Cognition and Neuroscience*, *34*(8), 949–972. https://doi.org/10.1080/23273798.2019.1608072

Fischl, B. (2012). FreeSurfer. *NeuroImage*, *62*(2), 774–781. https://doi.org/10.1016/j.neuroimage.2012.01.021

Fischl, B., van der Kouwe, A., Destrieux, C., Halgren, E., Ségonne, F., Salat, D. H., Busa, E., Seidman, L. J., Goldstein, J., Kennedy, D., Caviness, V., Makris, N., Rosen, B., & Dale, A. M. (2004). Automatically parcellating the human cerebral cortex. *Cerebral Cortex (New York, N.Y.: 1991)*, *14*(1), 11–22. https://doi.org/10.1093/cercor/bhg087

Fletcher, E., Gavett, B., Harvey, D., Farias, S. T., Olichney, J., Beckett, L., DeCarli, C., & Mungas, D. (2018). Brain Volume Change and Cognitive Trajectories in Aging. *Neuropsychology*, *32*(4), 436–449. https://doi.org/10.1037/neu0000447

Friederici, A. D. (2011). The Brain Basis of Language Processing: From Structure to Function. *Physiological Reviews*, *91*(4), 1357–1392. https://doi.org/10.1152/physrev.00006.2011

Friederici, A. D., Von Cramon, D. Y., & Kotz, S. A. (2007). Role of the Corpus Callosum in Speech Comprehension: Interfacing Syntax and Prosody. *Neuron*, *53*(1), 135–145. https://doi.org/10.1016/j.neuron.2006.11.020

Galbraith, S., Daniel, J. A., & Vissel, B. (2010). A Study of Clustered Data and Approaches to Its Analysis. *Journal of Neuroscience*, *30*(32), 10601–10608. https://doi.org/10.1523/JNEUROSCI.0362-10.2010

Gertel, V. H., Zhang, H., & Diaz, M. T. (2020). Stronger right hemisphere functional connectivity supports executive aspects of language in older adults. *Brain and Language*, *206*, 104771. https://doi.org/10.1016/j.bandl.2020.104771

Geva, S., Jones, P. S., Crinion, J. T., Price, C. J., Baron, J.-C., & Warburton, E. A. (2012). The Effect of Aging on the Neural Correlates of Phonological Word Retrieval. *Journal of Cognitive Neuroscience*, *24*(11), 2135–2146. https://doi.org/10.1162/jocn_a_00278

Goldstein, A., Covington, B. P., Mahabadi, N., & Mesfin, F. B. (2025). Neuroanatomy, Corpus Callosum. In *StatPearls*. StatPearls Publishing. http://www.ncbi.nlm.nih.gov/books/NBK448209/

Greenwood, P. M. (2000). The frontal aging hypothesis evaluated. *Journal of the International Neuropsychological Society*, *6*(6), 705–726. https://doi.org/10.1017/S1355617700666092

Greve, D. N., & Fischl, B. (2009). Accurate and robust brain image alignment using boundary-based registration. *NeuroImage*, *48*(1), 63–72. https://doi.org/10.1016/j.neuroimage.2009.06.060

Hagmann, P., Cammoun, L., Gigandet, X., Meuli, R., Honey, C. J., Wedeen, V. J., & Sporns, O. (2008). Mapping the Structural Core of Human Cerebral Cortex. *PLOS Biology*, *6*(7), e159. https://doi.org/10.1371/journal.pbio.0060159

Hallquist, M. N., Hwang, K., & Luna, B. (2013). The Nuisance of Nuisance Regression: Spectral Misspecification in a Common Approach to Resting-State fMRI Preprocessing Reintroduces Noise and Obscures Functional Connectivity. *NeuroImage*, *0*, 208–225. https://doi.org/10.1016/j.neuroimage.2013.05.116

Henriques, R. N., Henson, R., Cam-CAN, & Correia, M. M. (2023). Unique information from common diffusion MRI models about white-matter differences across the human adult lifespan. *Imaging Neuroscience*, *1*, 1–25. https://doi.org/10.1162/imag_a_00051

Henson, R., Büchel, C., Josephs, O., & Friston, K. (n.d.). *The Slice-Timing Problem in Event-related fMRI*.

Hou, J., & Pakkenberg, B. (2012). Age-related degeneration of corpus callosum in the 90+ years measured with stereology. *Neurobiology of Aging*, *33*(5), 1009.e1-1009.e9. https://doi.org/10.1016/j.neurobiolaging.2011.10.017

Houston, J., Allendorfer, J., Nenert, R., Goodman, A. M., & Szaflarski, J. P. (2019). White Matter Language Pathways and Language Performance in Healthy Adults Across Ages. *Frontiers in Neuroscience*, *13*. https://doi.org/10.3389/fnins.2019.01185

Huang, H., Zhang, J., Jiang, H., Wakana, S., Poetscher, L., Miller, M. I., van Zijl, P. CM., Hillis, A. E., Wytik, R., & Mori, S. (2005). DTI tractography based parcellation of white matter: Application to the mid-sagittal morphology of corpus callosum. *NeuroImage*, *26*(1), 195–205. https://doi.org/10.1016/j.neuroimage.2005.01.019

Jao, C., Yeh, J., Wu, Y.-T., Lien, L., Tsai, Y.-F., Chu, K.-E., Hsiao, C.-Y., Wang, P.-S., & Lau, C.-I. (2020). Alteration of the Intra- and Inter-Lobe Connectivity of the Brain Structural Network in Normal Aging. *Entropy*, *22*. https://doi.org/10.3390/e22080826

Jarret, J., Ferré, P., Chedid, G., Bedetti, C., Bore, A., Joanette, Y., Rouleau, I., & Maria Brambati, S. (2022). Functional network and structural connections involved in picture naming. *Brain and Language*, *231*, 105146. https://doi.org/10.1016/j.bandl.2022.105146

Jenkinson, M., Bannister, P., Brady, M., & Smith, S. (2002). Improved Optimization for the Robust and Accurate Linear Registration and Motion Correction of Brain Images. *NeuroImage*, *17*(2), 825–841. https://doi.org/10.1006/nimg.2002.1132

Jeurissen, B., Tournier, J.-D., Dhollander, T., Connelly, A., & Sijbers, J. (2014). Multi-tissue constrained spherical deconvolution for improved analysis of multi-shell diffusion MRI data. *NeuroImage*, *103*, 411–426. https://doi.org/10.1016/j.neuroimage.2014.07.061

Jiang, R., Scheinost, D., Zuo, N., Wu, J., Qi, S., Liang, Q., Zhi, D., Luo, N., Chung, Y., Liu, S., Xu, Y., Sui, J., & Calhoun, V. (2022). A Neuroimaging Signature of Cognitive Aging from Whole-Brain Functional Connectivity. *Advanced Science*, *9*(24), 2201621. https://doi.org/10.1002/advs.202201621

Jones, B. C., Nair, G., Shea, C. D., Crainiceanu, C. M., Cortese, I. C. M., & Reich, D. S. (2013). Quantification of multiple-sclerosis-related brain atrophy in two heterogeneous MRI datasets using mixed-effects modeling. *NeuroImage: Clinical*, *3*, 171–179. https://doi.org/10.1016/j.nicl.2013.08.001

Kellner, E., Dhital, B., Kiselev, V. G., & Reisert, M. (2016). Gibbs-ringing artifact removal based on local subvoxel-shifts. *Magnetic Resonance in Medicine*, *76*(5), 1574–1581. https://doi.org/10.1002/mrm.26054

Khalilian, M., Toba, M. N., Roussel, M., Tasseel-Ponche, S., Godefroy, O., & Aarabi, A. (2024). Age-related differences in structural and resting-state functional brain network organization across the adult lifespan: A cross-sectional study. *Aging Brain*, *5*, 100105. https://doi.org/10.1016/j.nbas.2023.100105

Knecht, S., Dräger, B., Deppe, M., Bobe, L., Lohmann, H., Flöel, A., Ringelstein, E.-B., & Henningsen, H. (2000). Handedness and hemispheric language dominance in healthy humans. *Brain*, *123*(12), 2512–2518. https://doi.org/10.1093/brain/123.12.2512

Kochunov, P., Thompson, P. M., Lancaster, J. L., Bartzokis, G., Smith, S., Coyle, T., Royall, D. R., Laird, A., & Fox, P. T. (2007). Relationship between white matter fractional anisotropy and other indices of cerebral health in normal aging: Tract-based spatial statistics study of aging. *NeuroImage*, *35*(2), 478–487. https://doi.org/10.1016/j.neuroimage.2006.12.021

Krüger, G., & Glover, G. H. (2001). Physiological noise in oxygenation-sensitive magnetic resonance imaging. *Magnetic Resonance in Medicine*, *46*(4), 631–637. https://doi.org/10.1002/mrm.1240

Kuznetsova, A., Brockhoff, P. B., & Christensen, R. H. B. (2017). lmerTest Package: Tests in Linear Mixed Effects Models. *Journal of Statistical Software*, *82*, 1–26. https://doi.org/10.18637/jss.v082.i13

Li, S.-C., Lindenberger, U., & Sikström, S. (2001). Aging cognition: From neuromodulation to representation. *Trends in Cognitive Sciences*, *5*(11), 479–486. https://doi.org/10.1016/S1364-6613(00)01769-1

Lin, X., & Zhang, D. (1999). Inference in Generalized Additive Mixed Models by Using Smoothing Splines. *Journal of the Royal Statistical Society Series B: Statistical Methodology*, *61*(2), 381–400. https://doi.org/10.1111/1467-9868.00183

Liu, C.-S. J., Miki, A., Hulvershorn, J., Bloy, L., Gualtieri, E. E., Liu, G. T., Leigh, J. S., Haselgrove, J. C., & Elliott, M. A. (2006). Spatial and Temporal Characteristics of Physiological Noise in fMRI at 3T. *Academic Radiology*, *13*(3), 313–323. https://doi.org/10.1016/j.acra.2005.10.018

Madden, D. J., Bennett, I. J., Burzynska, A., Potter, G. G., Chen, N., & Song, A. W. (2012). Diffusion Tensor Imaging of Cerebral White Matter Integrity in Cognitive Aging. *Biochimica et Biophysica Acta*, *1822*(3), 386–400. https://doi.org/10.1016/j.bbadis.2011.08.003

Madden, D. J., Jain, S., Monge, Z. A., Cook, A. D., Lee, A., Huang, H., Howard, C. M., & Cohen, J. R. (2020). Influence of structural and functional brain connectivity on age-related differences in fluid cognition. *Neurobiology of Aging*, *96*, 205–222. https://doi.org/10.1016/j.neurobiolaging.2020.09.010

Marrelec, G., Krainik, A., Duffau, H., Pélégrini-Issac, M., Lehéricy, S., Doyon, J., & Benali, H. (2006). Partial correlation for functional brain interactivity investigation in functional MRI. *NeuroImage*, *32*(1), 228–237. https://doi.org/10.1016/j.neuroimage.2005.12.057

Mascali, D., DiNuzzo, M., Serra, L., Mangia, S., Maraviglia, B., Bozzali, M., & Giove, F. (2018). Disruption of Semantic Network in Mild Alzheimer's Disease Revealed by Resting-State fMRI. *Neuroscience*, *371*, 38–48. https://doi.org/10.1016/j.neuroscience.2017.11.030

Muschelli, J., Nebel, M. B., Caffo, B. S., Barber, A. D., Pekar, J. J., & Mostofsky, S. H. (2014). Reduction of motion-related artifacts in resting state fMRI using aCompCor. *NeuroImage*, *96*, 22–35. https://doi.org/10.1016/j.neuroimage.2014.03.028

Naeser, M. A., Martin, P. I., Theoret, H., Kobayashi, M., Fregni, F., Nicholas, M., Tormos, J. M., Steven, M. S., Baker, E. H., & Pascual-Leone, A. (2011). TMS suppression of right pars triangularis, but not pars opercularis, improves naming in aphasia. *Brain and Language*, *119*(3), 206–213. https://doi.org/10.1016/j.bandl.2011.07.005

Naik, S., Banerjee, A., Bapi, R. S., Deco, G., & Roy, D. (2017). Metastability in Senescence. *Trends in Cognitive Sciences*, *21*(7), 509–521. https://doi.org/10.1016/j.tics.2017.04.007

Nilakantan, A. S., Voss, J. L., Weintraub, S., Mesulam, M.-M., & Rogalski, E. J. (2017). Selective verbal recognition memory impairments are associated with atrophy of the language network in non-semantic variants of primary progressive aphasia. *Neuropsychologia*, *100*, 10–17. https://doi.org/10.1016/j.neuropsychologia.2017.04.006

Papanicolaou, A. C., Kilintari, M., Rezaie, R., Narayana, S., & Babajani-Feremi, A. (2017). The Role of the Primary Sensory Cortices in Early Language Processing. *Journal of Cognitive Neuroscience*, *29*(10), 1755–1765. https://doi.org/10.1162/jocn_a_01147

Peelle, J. E., Chandrasekaran, K., Powers, J., Smith, E. E., & Grossman, M. (2013). Age-related vulnerability in the neural systems supporting semantic processing. *Frontiers in Aging Neuroscience*, *5*, 46. https://doi.org/10.3389/fnagi.2013.00046

Peelle, J. E., Troiani, V., Wingfield, A., & Grossman, M. (2010). Neural Processing during Older Adults' Comprehension of Spoken Sentences: Age Differences in Resource Allocation and Connectivity. *Cerebral Cortex (New York, NY)*, *20*(4), 773–782. https://doi.org/10.1093/cercor/bhp142

Pfefferbaum, A., Adalsteinsson, E., & Sullivan, E. V. (2005a). Frontal circuitry degradation marks healthy adult aging: Evidence from diffusion tensor imaging. *NeuroImage*, *26*(3), 891–899. https://doi.org/10.1016/j.neuroimage.2005.02.034

Pfefferbaum, A., Adalsteinsson, E., & Sullivan, E. V. (2005b). Frontal circuitry degradation marks healthy adult aging: Evidence from diffusion tensor imaging. *NeuroImage*, *26*(3), 891–899. https://doi.org/10.1016/j.neuroimage.2005.02.034

Pistono, A., Guerrier, L., Péran, P., Rafiq, M., Giméno, M., Bézy, C., Pariente, J., & Jucla, M. (2021). Increased functional connectivity supports language performance in healthy aging despite gray matter loss. *Neurobiology of Aging*, *98*, 52–62. https://doi.org/10.1016/j.neurobiolaging.2020.09.015

Price, C. J. (2010). The anatomy of language: A review of 100 fMRI studies published in 2009. *Annals of the New York Academy of Sciences*, *1191*(1), 62–88. https://doi.org/10.1111/j.1749-6632.2010.05444.x

Qi, T., Schaadt, G., & Friederici, A. D. (2019). Cortical thickness lateralization and its relation to language abilities in children. *Developmental Cognitive Neuroscience*, *39*, 100704. https://doi.org/10.1016/j.dcn.2019.100704

Rafiq, M., Jucla, M., Guerrier, L., Péran, P., Pariente, J., & Pistono, A. (2022). The functional connectivity of language network across the life span: Disentangling the effects of typical aging from Alzheimer's disease. *Frontiers in Aging Neuroscience*, *14*, 959405. https://doi.org/10.3389/fnagi.2022.959405

Rahul, D. R., & Joseph Ponniah, R. (2019). Language impairment in primary progressive aphasia and other neurodegenerative diseases. *Journal of Genetics*, *98*(4), 95. https://doi.org/10.1007/s12041-019-1139-5

Reuter-Lorenz, P. A., & Cappell, K. A. (2008). Neurocognitive Aging and the Compensation Hypothesis. *Current Directions in Psychological Science*, *17*(3), 177–182. https://doi.org/10.1111/j.1467-8721.2008.00570.x

Riha, C., Güntensperger, D., Kleinjung, T., & Meyer, M. (2020). Accounting for Heterogeneity: Mixed-Effects Models in Resting-State EEG Data in a Sample of Tinnitus Sufferers. *Brain Topography*, *33*(4), 413–424. https://doi.org/10.1007/s10548-020-00772-7

Roger, E., Labache, L., Hamlin, N., Kruse, J., Baciu, M., & Doucet, G. E. (2023). When Age Tips the Balance: A Dual Mechanism Affecting Hemispheric Specialization for Language. *bioRxiv*, 2023.12.04.569978. https://doi.org/10.1101/2023.12.04.569978

Salat, D. H., Tuch, D. S., Greve, D. N., van der Kouwe, A. J. W., Hevelone, N. D., Zaleta, A. K., Rosen, B. R., Fischl, B., Corkin, S., Rosas, H. D., & Dale, A. M. (2005). Age-related alterations in white matter microstructure measured by diffusion tensor imaging. *Neurobiology of Aging*, *26*(8), 1215–1227. https://doi.org/10.1016/j.neurobiolaging.2004.09.017

Salthouse, T. A. (2014). Quantity and structure of word knowledge across adulthood. *Intelligence*, *46*, 122–130.

Scandola, M., & Tidoni, E. (2021). *Reliability and feasibility of Linear Mixed Models in fully crossed experimental designs*. https://doi.org/10.31234/osf.io/kfhgv

Shafto, M. A., Burke, D. M., Stamatakis, E. A., Tam, P. P., & Tyler, L. K. (2007). On the Tip-of-the-Tongue: Neural Correlates of Increased Word-finding Failures in Normal Aging. *Journal of Cognitive Neuroscience*, *19*(12), 2060–2070. https://doi.org/10.1162/jocn.2007.19.12.2060

Shafto, M. A., & Tyler, L. K. (2014). Language in the aging brain: The network dynamics of cognitive decline and preservation. *Science*, *346*(6209), 583–587. https://doi.org/10.1126/science.1254404

Shafto, M. A., Tyler, L. K., Dixon, M., Taylor, J. R., Rowe, J. B., Cusack, R., Calder, A. J., Marslen-Wilson, W. D., Duncan, J., Dalgleish, T., Henson, R. N., Brayne, C., & Matthews, F. E. (2014). The Cambridge Centre for Ageing and Neuroscience (Cam-CAN) study protocol: A cross-sectional, lifespan, multidisciplinary examination of healthy cognitive ageing. *BMC Neurology*, *14*, 204. https://doi.org/10.1186/s12883-014-0204-1

Smith, R. E., Tournier, J.-D., Calamante, F., & Connelly, A. (2012). Anatomically-constrained tractography: Improved diffusion MRI streamlines tractography through effective use of anatomical information. *NeuroImage*, *62*(3), 1924–1938. https://doi.org/10.1016/j.neuroimage.2012.06.005

Smith, R. E., Tournier, J.-D., Calamante, F., & Connelly, A. (2015). SIFT2: Enabling dense quantitative assessment of brain white matter connectivity using streamlines tractography. *NeuroImage*, *119*, 338–351. https://doi.org/10.1016/j.neuroimage.2015.06.092

Smith, S. M., Jenkinson, M., Woolrich, M. W., Beckmann, C. F., Behrens, T. E. J., Johansen-Berg, H., Bannister, P. R., De Luca, M., Drobnjak, I., Flitney, D. E., Niazy, R. K., Saunders, J., Vickers, J., Zhang, Y., De Stefano, N., Brady, J. M., & Matthews, P. M. (2004). Advances in functional and structural MR image analysis and implementation as FSL. *NeuroImage*, *23 Suppl 1*, S208-219. https://doi.org/10.1016/j.neuroimage.2004.07.051

Smith, S. M., Miller, K. L., Salimi-Khorshidi, G., Webster, M., Beckmann, C. F., Nichols, T. E., Ramsey, J. D., & Woolrich, M. W. (2011). Network modelling methods for FMRI. *NeuroImage*, *54*(2), 875–891. https://doi.org/10.1016/j.neuroimage.2010.08.063

Sommers, M. S., Hale, S., Myerson, J., Rose, N., Tye-Murray, N., & Spehar, B. (2011). Listening Comprehension Across the Adult Lifespan. *Ear and Hearing*, *32*(6), 775. https://doi.org/10.1097/AUD.0b013e3182234cf6

Sørensen, Ø., Brandmaier, A. M., Macià, D., Ebmeier, K., Ghisletta, P., Kievit, R. A., Mowinckel, A. M., Walhovd, K. B., Westerhausen, R., & Fjell, A. (2021). Meta-analysis of generalized additive models in neuroimaging studies. *NeuroImage*, *224*, 117416. https://doi.org/10.1016/j.neuroimage.2020.117416

Sørensen, Ø., Walhovd, K. B., & Fjell, A. M. (2021). A recipe for accurate estimation of lifespan brain trajectories, distinguishing longitudinal and cohort effects. *NeuroImage*, *226*, 117596. https://doi.org/10.1016/j.neuroimage.2020.117596

Sullivan, E. V., Rohlfing, T., & Pfefferbaum, A. (2010). Quantitative fiber tracking of lateral and interhemispheric white matter systems in normal aging. *Neurobiology of Aging*, *31*(3), 464. https://doi.org/10.1016/j.neurobiolaging.2008.04.007

Taylor, J. R., Williams, N., Cusack, R., Auer, T., Shafto, M. A., Dixon, M., Tyler, L. K., Cam-CAN, & Henson, R. N. (2017). The Cambridge Centre for Ageing and Neuroscience (Cam-CAN) data repository: Structural and functional MRI, MEG, and cognitive data from a cross-sectional adult lifespan sample. *Neuroimage*, *144*(Pt B), 262–269. https://doi.org/10.1016/j.neuroimage.2015.09.018

Tejavibulya, L., Peterson, H., Greene, A., Gao, S., Rolison, M., Noble, S., & Scheinost, D. (2022). Large-scale differences in functional organization of left- and right-handed individuals using whole-brain, data-driven analysis of connectivity. *NeuroImage*, *252*, 119040. https://doi.org/10.1016/j.neuroimage.2022.119040

The Florey Institute of Neuroscience and Mental Health, Smith, R. E., Florey Department of Neuroscience and Mental Health, University of Melbourne, Raffelt, D., The Florey Institute of Neuroscience and Mental Health, Tournierc, J.-D., Centre for the Developing Brain, School of Biomedical Engineering & Imaging Sciences, Connelly, A., The Florey Institute of Neuroscience and Mental Health, Florey Department of Neuroscience and Mental Health, University of Melbourne, & Department of Medicine, Austin Health and Northern Health, University of Melbourne. (2022). Quantitative streamlines tractography: Methods and inter-subject normalisation. *Aperture Neuro*, 1–25. https://doi.org/10.52294/ApertureNeuro.2022.2.NEOD9565

Tournier, J.-D., Smith, R., Raffelt, D., Tabbara, R., Dhollander, T., Pietsch, M., Christiaens, D., Jeurissen, B., Yeh, C.-H., & Connelly, A. (2019). MRtrix3: A fast, flexible and open software framework for medical image processing and visualisation. *NeuroImage*, *202*, 116137. https://doi.org/10.1016/j.neuroimage.2019.116137

Tournier, J.-D., Yeh, C.-H., Calamante, F., Cho, K.-H., Connelly, A., & Lin, C.-P. (2008). Resolving crossing fibres using constrained spherical deconvolution: Validation using diffusion-weighted imaging phantom data. *NeuroImage*, *42*(2), 617–625. https://doi.org/10.1016/j.neuroimage.2008.05.002

Tustison, N. J., Avants, B. B., Cook, P. A., Zheng, Y., Egan, A., Yushkevich, P. A., & Gee, J. C. (2010). N4ITK: Improved N3 bias correction. *IEEE Transactions on Medical Imaging*, *29*(6), 1310–1320. https://doi.org/10.1109/TMI.2010.2046908

Tyler, L. K., Shafto, M. A., Randall, B., Wright, P., Marslen-Wilson, W. D., & Stamatakis, E. A. (2010). Preserving Syntactic Processing across the Adult Life Span: The Modulation of the Frontotemporal Language System in the Context of Age-Related Atrophy. *Cerebral Cortex (New York, NY)*, *20*(2), 352–364. https://doi.org/10.1093/cercor/bhp105

Uddin, L. Q. (2021). Cognitive and behavioural flexibility: Neural mechanisms and clinical considerations. *Nature Reviews Neuroscience*, *22*(3), 167–179. https://doi.org/10.1038/s41583-021-00428-w

United Nations (Ed.). (2023). *Leaving no one behind in an ageing world*. United Nations.

van Boxtel, W., & Lawyer, L. (2021). Sentence comprehension in ageing and Alzheimer's disease. *Language and Linguistics Compass*, *15*(6), e12430. https://doi.org/10.1111/lnc3.12430

Veraart, J., Novikov, D. S., Christiaens, D., Ades-Aron, B., Sijbers, J., & Fieremans, E. (2016). Denoising of diffusion MRI using random matrix theory. *NeuroImage*, *142*, 394–406. https://doi.org/10.1016/j.neuroimage.2016.08.016

Verhaegen, C., & Poncelet, M. (2013). Changes in Naming and Semantic Abilities With Aging From 50 to 90 years. *Journal of the International Neuropsychological Society*, *19*(2), 119–126. https://doi.org/10.1017/S1355617712001178

Wang, P., Meng, C., Yuan, R., Wang, J., Yang, H., Zhang, T., Zaborszky, L., Alvarez, T. L., Liao, W., Luo, C., Chen, H., & Biswal, B. B. (2020). The Organization of the Human Corpus Callosum Estimated by Intrinsic Functional Connectivity with White-Matter Functional Networks. *Cerebral Cortex*, *30*(5), 3313–3324. https://doi.org/10.1093/cercor/bhz311

Westlye, L. T., Walhovd, K. B., Dale, A. M., Bjørnerud, A., Due-Tønnessen, P., Engvig, A., Grydeland, H., Tamnes, C. K., Østby, Y., & Fjell, A. M. (2010). Life-Span Changes of the Human Brain White Matter: Diffusion Tensor Imaging (DTI) and Volumetry. *Cerebral Cortex*, *20*(9), 2055–2068. https://doi.org/10.1093/cercor/bhp280

Whitfield-Gabrieli, S., & Nieto-Castanon, A. (2012). Conn: A Functional Connectivity Toolbox for Correlated and Anticorrelated Brain Networks. *Brain Connectivity*, *2*, 125–141. https://doi.org/10.1089/brain.2012.0073

Wickham, H. (2016). Programming with ggplot2. In H. Wickham (Ed.), *Ggplot2: Elegant Graphics for Data Analysis* (pp. 241–253). Springer International Publishing. https://doi.org/10.1007/978-3-319-24277-4_12

Wilson, S. M., Galantucci, S., Tartaglia, M. C., Rising, K., Patterson, D. K., Henry, M. L., Ogar, J. M., DeLeon, J., Miller, B. L., & Gorno-Tempini, M. L. (2011). Syntactic processing depends on dorsal language tracts. *Neuron*, *72*(2), 397–403. https://doi.org/10.1016/j.neuron.2011.09.014

Wood, S. N. (2017). *Generalized Additive Models: An Introduction with R, Second Edition* (2nd ed.). Chapman and Hall/CRC. https://doi.org/10.1201/9781315370279

Woolrich, M. W., Jbabdi, S., Patenaude, B., Chappell, M., Makni, S., Behrens, T., Beckmann, C., Jenkinson, M., & Smith, S. M. (2009). Bayesian analysis of neuroimaging data in FSL. *NeuroImage*, *45*(1, Supplement 1), S173–S186. https://doi.org/10.1016/j.neuroimage.2008.10.055

Xia, M., Wang, J., & He, Y. (2013). BrainNet Viewer: A Network Visualization Tool for Human Brain Connectomics. *PLoS ONE*, *8*(7), e68910. https://doi.org/10.1371/journal.pone.0068910

Yang, Y., Dai, B., Howell, P., Wang, X., Li, K., & Lu, C. (2014). White and Grey Matter Changes in the Language Network during Healthy Aging. *PLoS ONE*, *9*(9), e108077. https://doi.org/10.1371/journal.pone.0108077

Zalesky, A., Fornito, A., & Bullmore, E. (2012). On the use of correlation as a measure of network connectivity. *NeuroImage*, *60*(4), 2096–2106. https://doi.org/10.1016/j.neuroimage.2012.02.001

Zhang, H., Bai, X., & Diaz, M. T. (2021). The intensity and connectivity of spontaneous brain activity in a language network relate to aging and language. *Neuropsychologia*, *154*, 107784. https://doi.org/10.1016/j.neuropsychologia.2021.107784

Zhang, H., & Diaz, M. T. (2023a). Resting State Network Segregation Modulates Age-Related Differences in Language Production. *Neurobiology of Language (Cambridge, Mass.)*, *4*(2), 382–403. https://doi.org/10.1162/nol_a_00106

Zhang, H., & Diaz, M. T. (2023b). Task difficulty modulates age-related differences in functional connectivity during word production. *Brain and Language*, *240*, 105263. https://doi.org/10.1016/j.bandl.2023.105263

Figure Captions:

Figure 1. A, Three-dimensional representation of LAN ROIs (Regions of Interest) in both hemispheres, shown from medial and lateral views. B, Distribution of age (18-88) among 558 CamCAN participants. C, Age-related variation in language task performance depicted through horizontal bar plots. Each bar represents the beta coefficient for age across different language comprehension and production tasks derived from the Linear mixed model (LME; Equation 1), color-coded based on significance levels. Abbreviations: ParsO (Pars Opercularis), ParsT (Pars Triangularis), MTG (Middle Temporal Gyrus), STG (Superior Temporal Gyrus), STS (Superior Temporal Sulcus), Vocab (Vocabulary), ToT (Tip of the Tongue), VF (Verbal Fluency), High_phon (High Phonetic Similarity), High_sem (High Semantic Similarity), Low_phon (Low Phonetic Similarity), Low_sem (Low Semantic Similarity), RT (Response Time), Syn_comp (Syntactically Complex), and Sem_comp (Semantically Complex).

Figure 2. Age-related variation in structural connectivity within the language network across intra- and inter-hemispheric pathways. Beta estimates from linear mixed-effects models (LMEs; Equation 4) are visualized for 45 language network (LAN) edges to quantify the effect of age on structural connectivity (SC). Panels A–C represent results for left-hemispheric (A), right-hemispheric (B), and inter-hemispheric (C) connections, respectively. Each horizontal bar corresponds to an individual edge, with the x-axis reflecting the estimated fixed effect of age on SC strength. Significance levels are indicated by bar shading: dark blue for $p < 0.001$, medium blue for $p < 0.01$, light blue for $p < 0.05$, and grey for non-significant results (FDR-corrected). Central schematics represent the spatial distribution of connections across the LAN, with edges coloured according to the signed beta coefficient, consistent with the colour bar scale. Labels “L” and “R” denote left and right hemispheres, respectively. All region abbreviations are consistent with those presented in Figure 1.

Figure 3. Age-related variation in functional connectivity within the language network across intra- and inter-hemispheric pathways. Panels A–C display fixed-effect estimates for age on functional connectivity (FC) within the language network (LAN), derived from linear mixed-effects modeling (LMEs; Equation 6). Panel A shows left-hemispheric connections, Panel B right-hemispheric connections, and Panel C inter-hemispheric connections. Bars represent the magnitude and direction of the age coefficient for each LAN edge. Significance levels are color-coded following FDR correction: dark blue = $p < 0.001$, medium blue = $p < 0.01$, light blue = $p < 0.05$, grey = non-significant. Central schematic brain plots provide spatial context for each edge, with edges coloured by beta coefficient magnitude and direction as indicated by the continuous scale below. Labels “L” and “R” denote left and right hemispheres, respectively. All region abbreviations are consistent with those presented in Figure 1.

Figure 4. Differential non-linear age-related modulation of language behavior by edge-specific structural and functional connectivity within the language network. (A–B) Heatmaps display estimated degrees of freedom (edf) from Generalized Additive Mixed Models (GAMMs; Equations 7 and 8), capturing non-linear interaction effects between age and edge-specific structural connectivity (SC; A) and functional connectivity (FC; B) across 45 language network edges and 16 language behavior tasks. Blue squares indicate significant interactions (FDR-corrected $p < 0.05$) with edf > 2, where darker shades reflect stronger non-linearity. Grey squares represent non-significant interactions. (C–D) Corresponding F-statistic heatmaps from post-hoc ANOVA comparisons between the full interaction models (Equations 7 and 8) and a baseline age-only model (Equation 9). Blue squares mark robust edge-wise interactions that remain significant after accounting for general age effects (FDR-corrected $p < 0.05$), for SC (C) and FC (D), respectively. Edges are color-coded by hemispheric organization: Left-hemispheric (blue), Right-hemispheric (orange), and Inter-hemispheric (purple). Language tasks are grouped by domain: comprehension (green) and production (red). Edge abbreviations are provided in Figure 1.

Figure 5. Differential lifespan modulation of language comprehension and production by edge-specific connectivity strength across the language network. Panels A–D illustrate predicted behavioral trajectories from Generalized Additive Mixed Models (GAMMs; Equations 7 and 8) for representative SC × age (A–B) and FC × age (C–D) interactions, derived from significant edges identified from post-hoc ANOVA comparisons (see Figure 4). Each panel represents a distinct combination of connection modality and language domain: structural connectivity (SC) in comprehension (A) and production (B) tasks, and functional connectivity (FC) in comprehension (C) and production (D) tasks. Within each subplot, GAMM-derived trajectories depict language performance across the adult lifespan (18–88 years) at three quantiles of connectivity strength: low (0.25, red line), medium (0.50, grey line), and high (0.75, blue line). The y-axis represents the predicted behavioral outcome for each task. Accompanying brain schematics denote the anatomical location and edges are color-coded by modality, with red denoting SC and blue for FC. Anatomical region abbreviations are consistent with those presented in Figure 1.

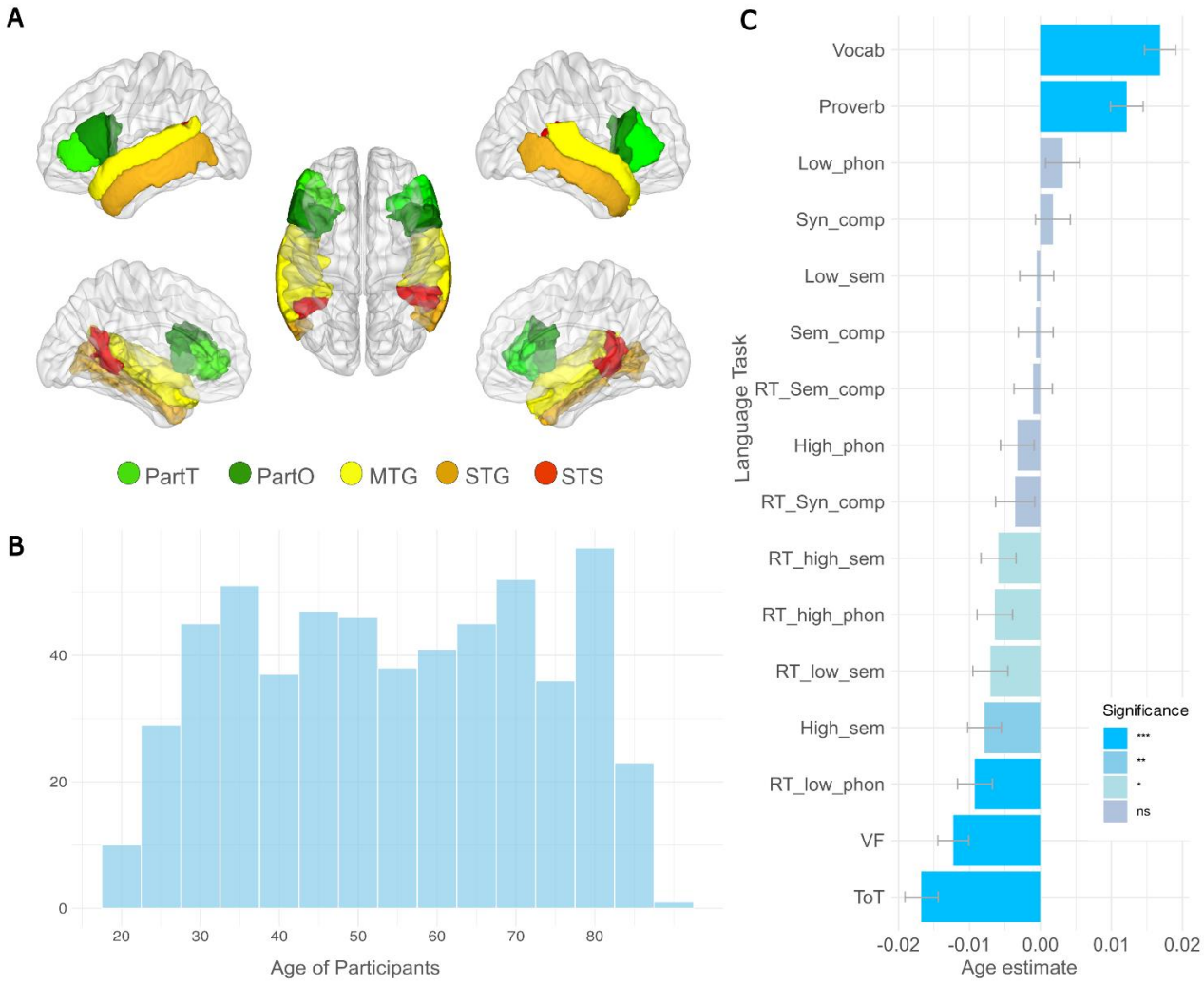
A
PartT
PartO
MTG
STG
STS
B
40
20
0
20
30
40
50
60
70
80
Age of Participants
C
Vocab
Proverb
Low_phon
Syn_comp
Low_sem
Sem_comp
RT_Sem_comp
High_phon
RT_Syn_comp
RT_high_sem
RT_high_phon
RT_low_sem
High_sem
RT_low_phon
VF
ToT
Language Task
-0.02
-0.01
0.00
0.01
0.02
Age estimate
Significance
***
**
*
ns

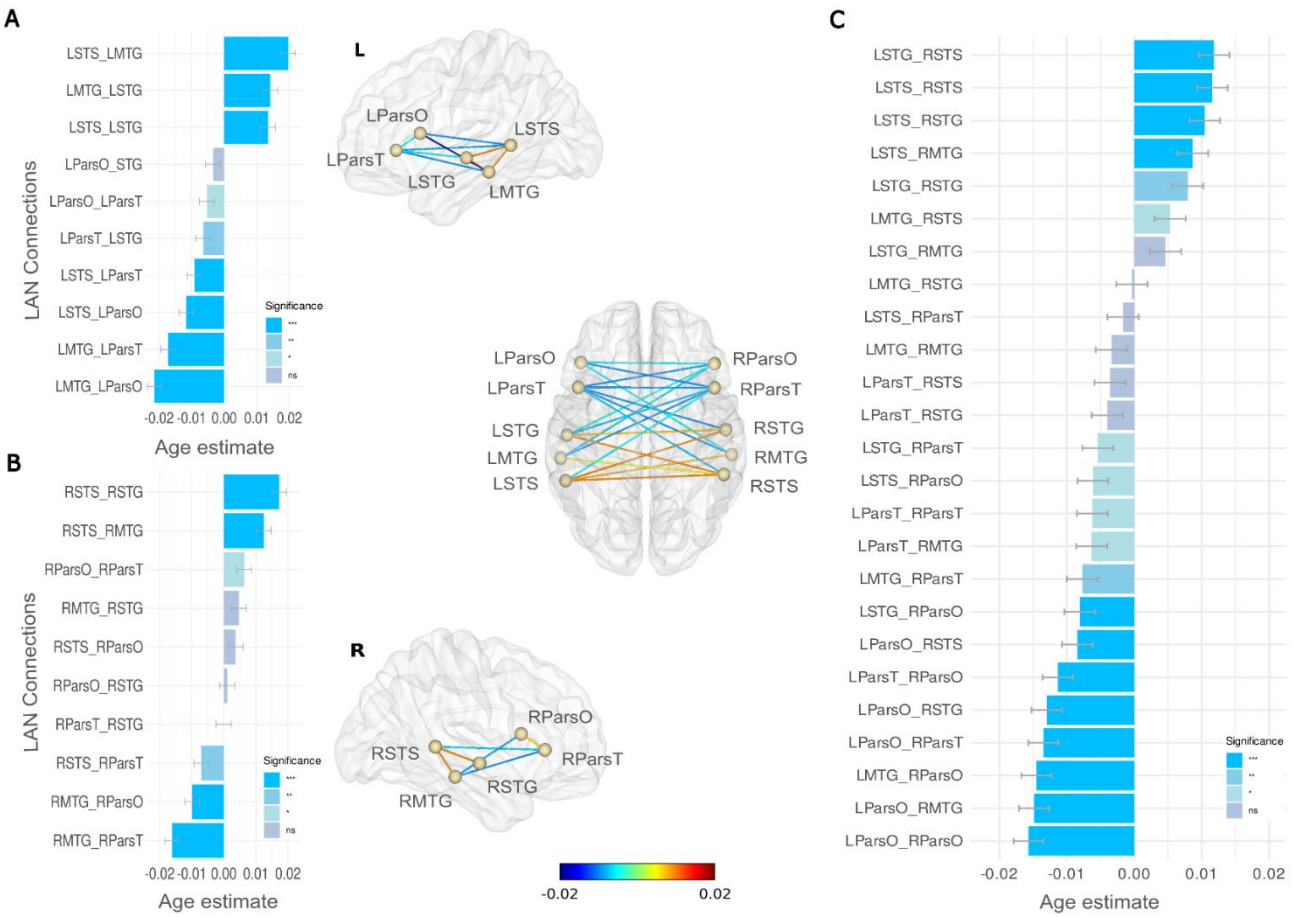
A
LSTS_LMTG
LMTG_LSTG
LSTS_LSTG
LParsO_STG
LParsO_LParsT
LParsT_LSTG
LSTS_LParsT
LSTS_LParsO
LMTG_LParsT
LMTG_LParsO
LAN Connections
Significance
***
**
*
ns
-0.02 -0.01 0.00 0.01 0.02
Age estimate
B
RSTS_RSTG
RSTS_RMTG
RParsO_RParsT
RMTG_RSTG
RSTS_RParsO
RParsO_RSTG
RParsT_RSTG
RSTS_RParsT
RMTG_RParsO
RMTG_RParsT
LAN Connections
Significance
***
**
*
ns
-0.02 -0.01 0.00 0.01 0.02
Age estimate
L
LParsO
LSTS
LParsT
LSTG
LMTG
LParsO
RParsO
LParsT
RParsT
LSTG
RSTG
LMTG
RMTG
LSTS
RSTS
R
RParsO
RSTS
RParsT
RSTG
RMTG
-0.02
0.02
C
LSTG_RSTS
LSTS_RSTS
LSTS_RSTG
LSTS_RMTG
LSTG_RSTG
LMTG_RSTS
LSTG_RMTG
LMTG_RSTG
LSTS_RParsT
LMTG_RMTG
LParsT_RSTS
LParsT_RSTG
LSTG_RParsT
LSTS_RParsO
LParsT_RParsT
LParsT_RMTG
LMTG_RParsT
LSTG_RParsO
LParsO_RSTS
LParsT_RParsO
LParsO_RSTG
LParsO_RParsT
LMTG_RParsO
LParsO_RMTG
LParsO_RParsO
Significance
***
**
*
ns
-0.02 -0.01 0.00 0.01 0.02
Age estimate

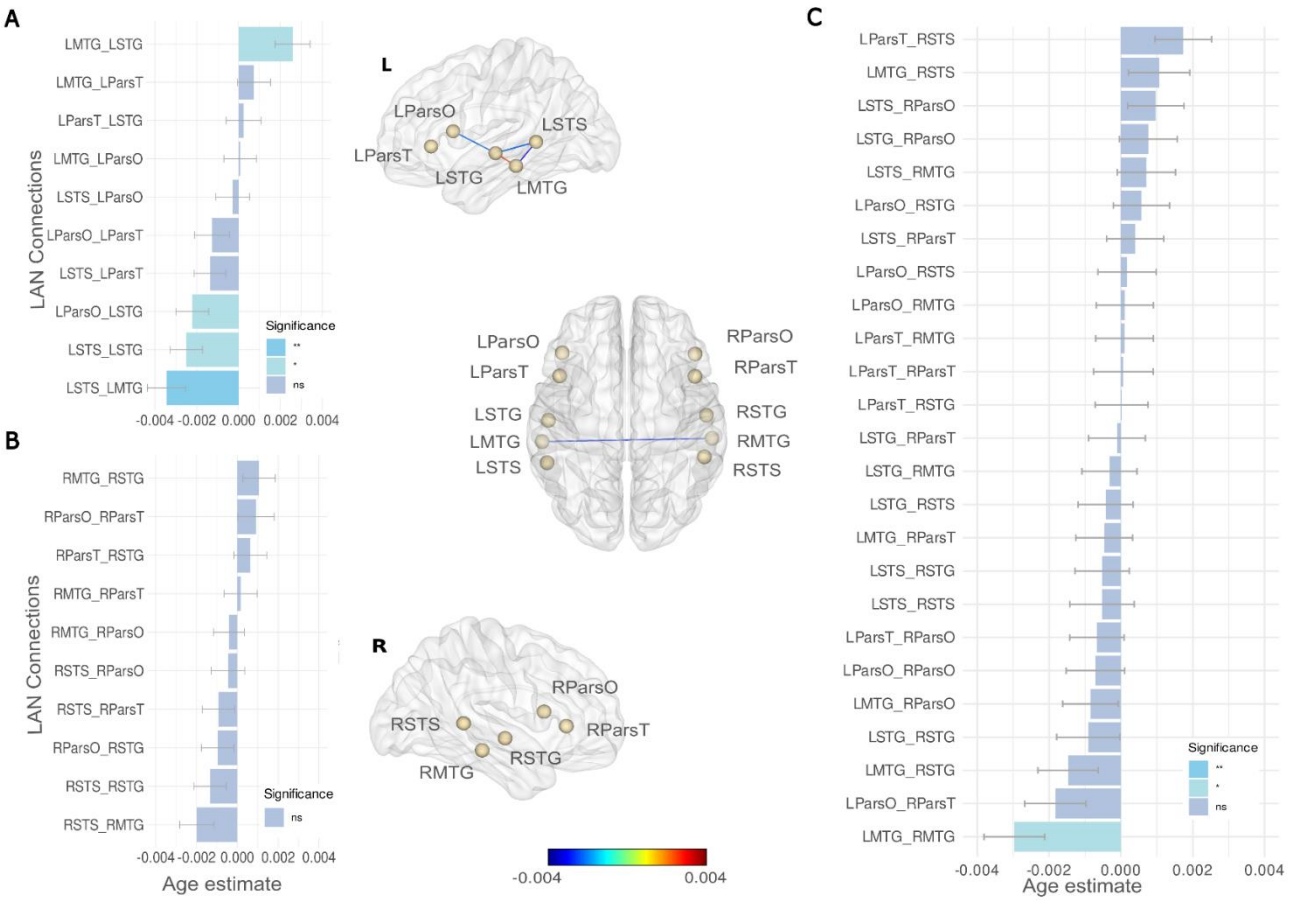
A
LMTG_LSTG
LMTG_LParsT
LParsT_LSTG
LMTG_LParsO
LSTS_LParsO
LParsO_LParsT
LSTS_LParsT
LParsO_LSTG
LSTS_LSTG
LSTS_LMTG
LAN Connections
Significance
**
*
ns
-0.004 -0.002 0.000 0.002 0.004
B
RMTG_RSTG
RParsO_RParsT
RParsT_RSTG
RMTG_RParsT
RMTG_RParsO
RSTS_RParsO
RSTS_RParsT
RParsO_RSTG
RSTS_RSTG
RSTS_RMTG
LAN Connections
Significance
ns
-0.004 -0.002 0.000 0.002 0.004
Age estimate
L
LParsO
LSTS
LParsT
LSTG
LMTG
LParsO
RParsO
LParsT
RParsT
LSTG
RSTG
LMTG
RMTG
LSTS
RSTS
R
RParsO
RSTS
RParsT
RSTG
RMTG
-0.004
0.004
C
LParsT_RSTS
LMTG_RSTS
LSTS_RParsO
LSTG_RParsO
LSTS_RMTG
LParsO_RSTG
LSTS_RParsT
LParsO_RSTS
LParsO_RMTG
LParsT_RMTG
LParsT_RParsT
LParsT_RSTG
LSTG_RParsT
LSTG_RMTG
LSTG_RSTS
LMTG_RParsT
LSTS_RSTG
LSTS_RSTS
LParsT_RParsO
LParsO_RParsO
LMTG_RParsO
LSTG_RSTG
LMTG_RSTG
LParsO_RParsT
LMTG_RMTG
Significance
**
*
ns
-0.004 -0.002 0.000 0.002 0.004
Age estimate

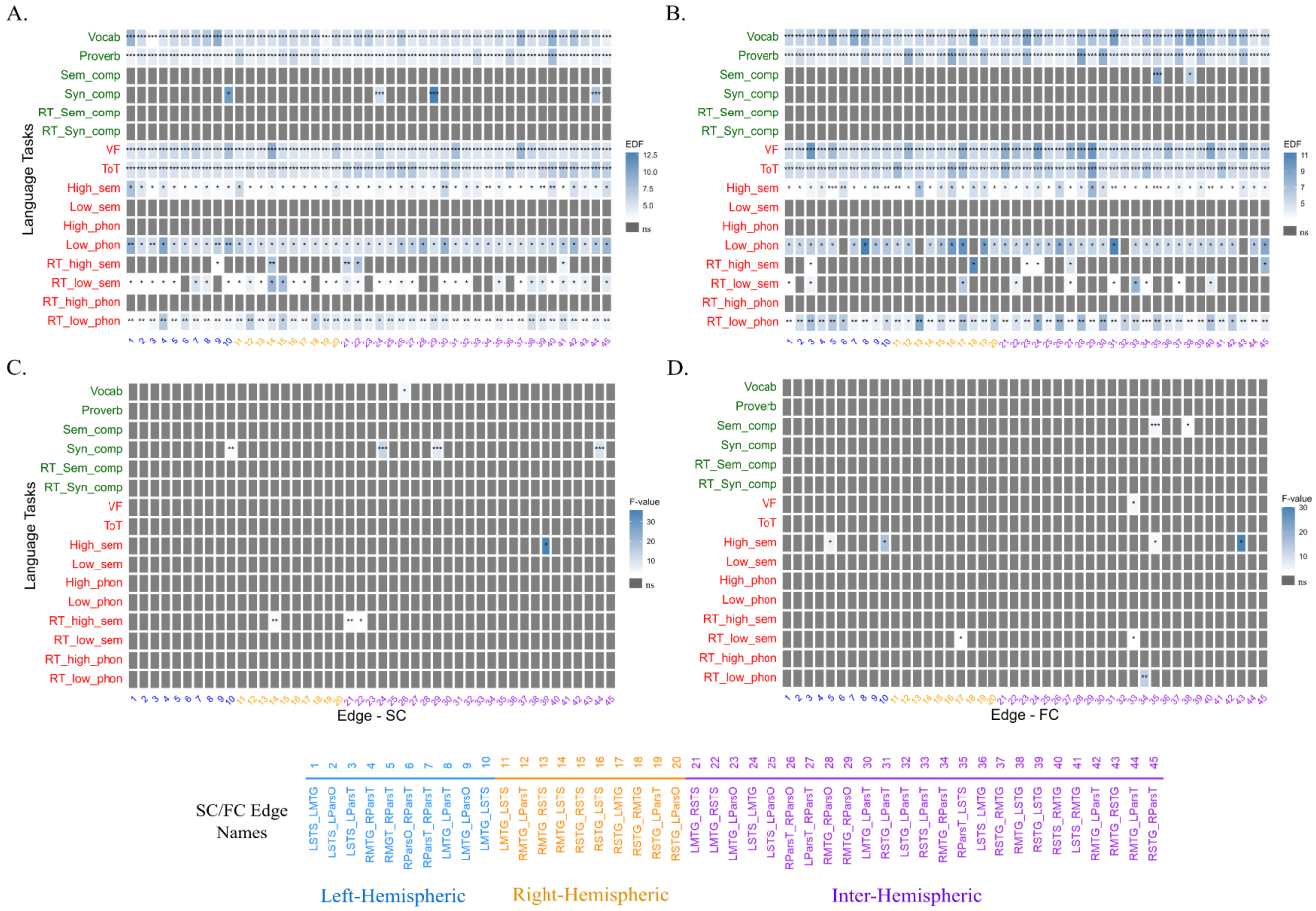
A.
B.
C.
D.
Vocab
Proverb
Sem_comp
Syn_comp
RT_Sem_comp
RT_Syn_comp
VF
ToT
High_sem
Low_sem
High_phon
Low_phon
RT_high_sem
RT_low_sem
RT_high_phon
RT_low_phon
Language Tasks
EDF
F-value
ns
Edge - SC
Edge - FC

SC/FC Edge Names
1 LSTS_LMTG
2 LSTS_LParsO
3 LSTS_LParsT
4 RMTG_RParsT
5 RMGT_RParsT
6 RParsO_RParsT
7 RParsT_RParsT
8 LMTG_LParsT
9 LMTG_LParsO
10 LMTG_LSTS
11 LMTG_LSTS
12 RMTG_LParsT
13 RMTG_RSTS
14 RMTG_LSTS
15 RSTG_RSTS
16 RSTG_LSTS
17 RSTG_LMTG
18 RSTG_RMTG
19 RSTG_LParsT
20 RSTG_LParsO
21 LMTG_RSTS
22 LMTG_RSTS
23 LMTG_LParsO
24 LSTS_LMTG
25 LSTS_LParsO
26 RParsT_RParsO
27 LParsT_RParsT
28 RMTG_RParsO
29 RMTG_RParsO
30 LMTG_LParsT
31 RSTG_LParsT
32 LSTG_LParsT
33 RSTS_LParsT
34 RMTG_RParsT
35 RParsT_LSTS
36 LSTS_LMTG
37 RSTG_RMTG
38 RMTG_LSTG
39 RSTG_LSTG
40 RSTS_RMTG
41 LSTS_RMTG
42 RMTG_LParsT
43 RMTG_RSTG
44 RMTG_LParsT
45 RSTG_RParsT
Left-Hemispheric
Right-Hemispheric
Inter-Hemispheric

A. SC - Comprehension tasks

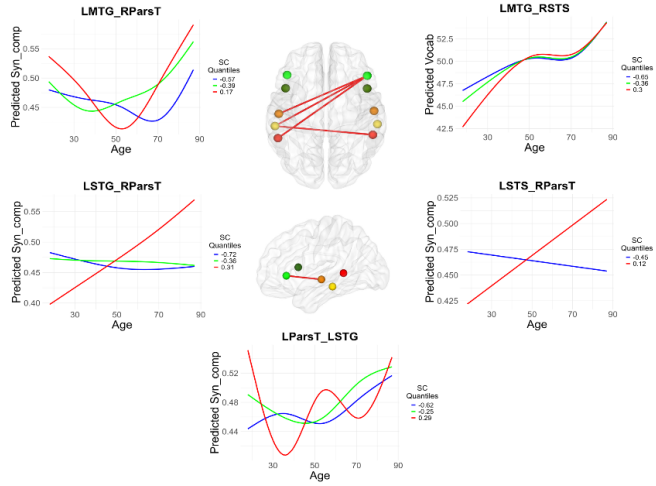

B. SC - Production tasks

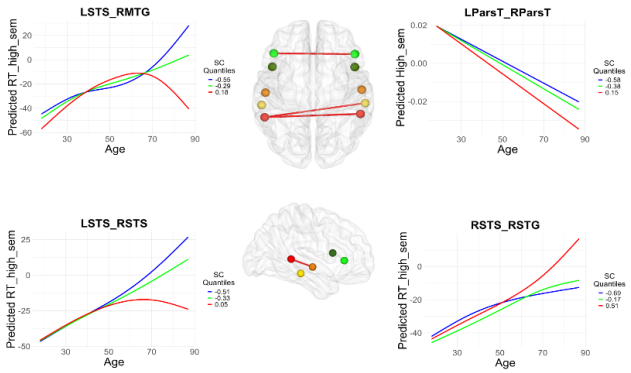

C. FC - Comprehension tasks

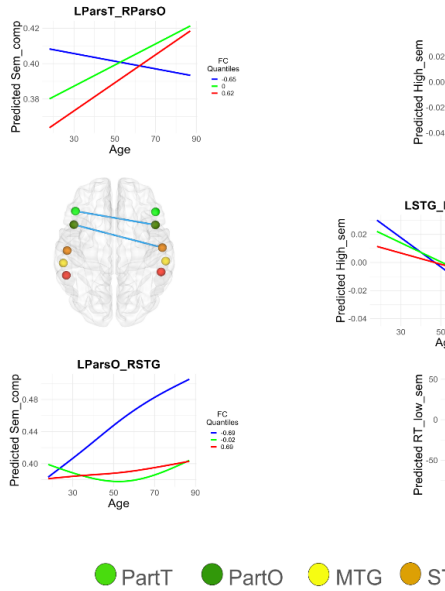
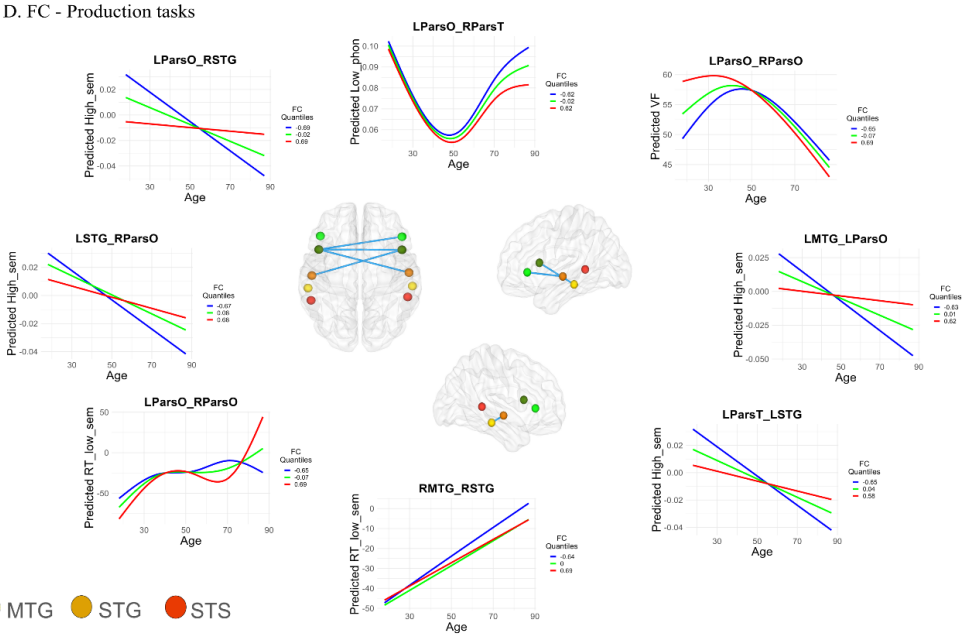
D. FC - Production tasks